



I JORNADAS DE DIFUSION DE LOS CENTROS
DE APOYO A LA INVESTIGACION UCM
24/10/2016



Investigación aplicada en Ciencias de la Tierra: Técnicas y tecnologías de interés

María Josefa Herrero Fernández
Dpto. de Petrología y Geoquímica
Facultad de Ciencias Geológicas, UCM

NOT CROSS

CRIME SCENE - DO NOT CROSS

CRIME SC

Concreciones en edificio
de San Sebastián



Análisis de Actividad de
Fallas



2



Trabajo de Campo



Análisis de Laboratorio

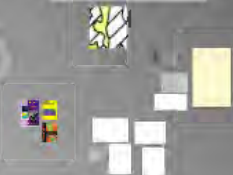


Y una vez resuelto
el misterio...



3

Del Clima del Pasado
al Clima del Futuro

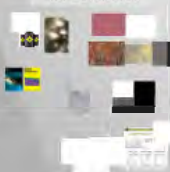


4

ATC
Almacén Temporal Centralizado
de Residuos Nucleares



Exploración de
hidrocarburos



1

2345

12345



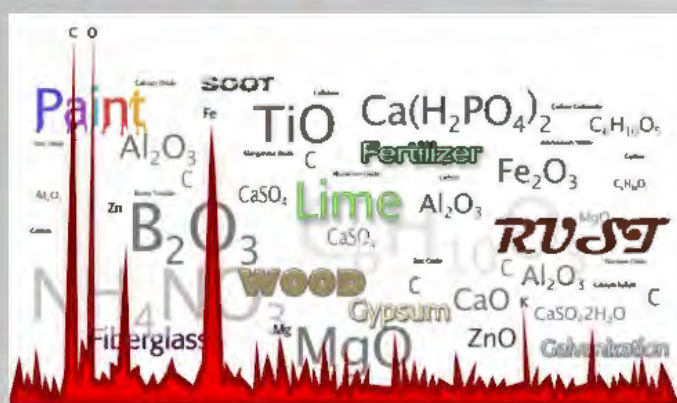
Trabajo de Campo



Análisis de Laboratorio



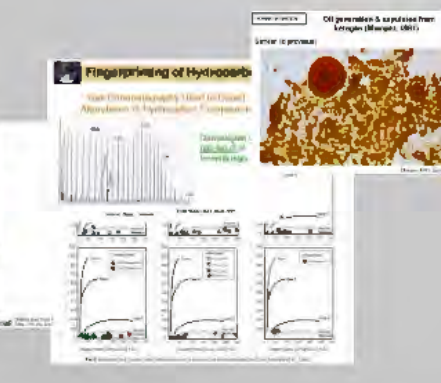
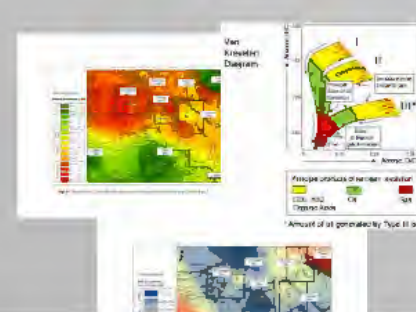
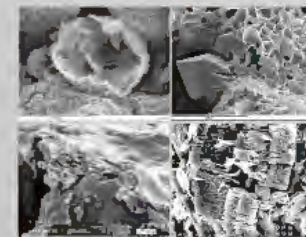
CAI Técnicas Geológicas



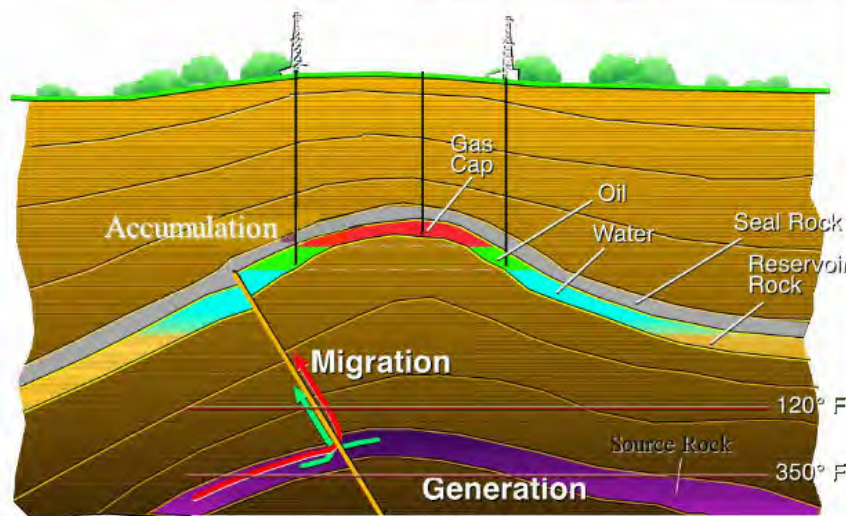
Y una vez resuelto el misterio...



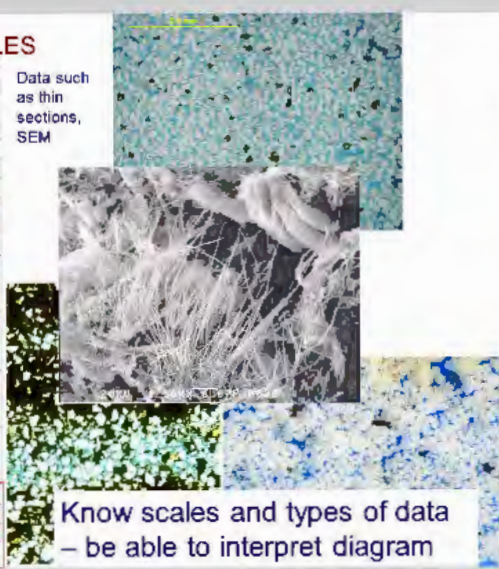
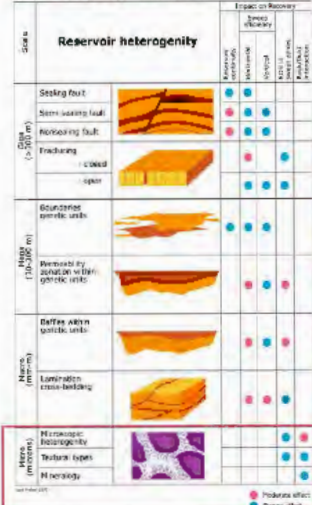
Exploración de hidrocarburos



Petroleum System Elements and Processes

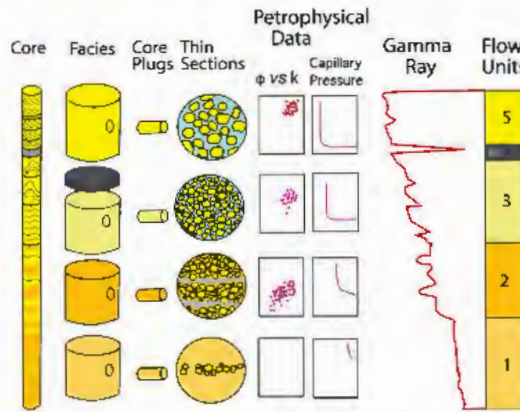


HETEROGENEITY ▶ SCALES



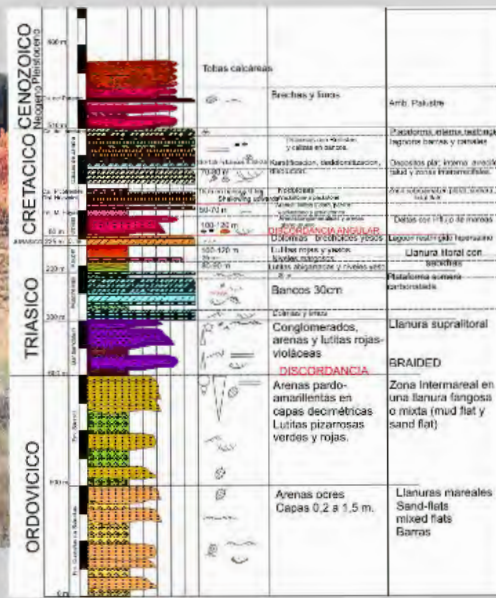
HETEROGENEITY ▶ CHARACTERIZATION ▶ FLOW UNITS

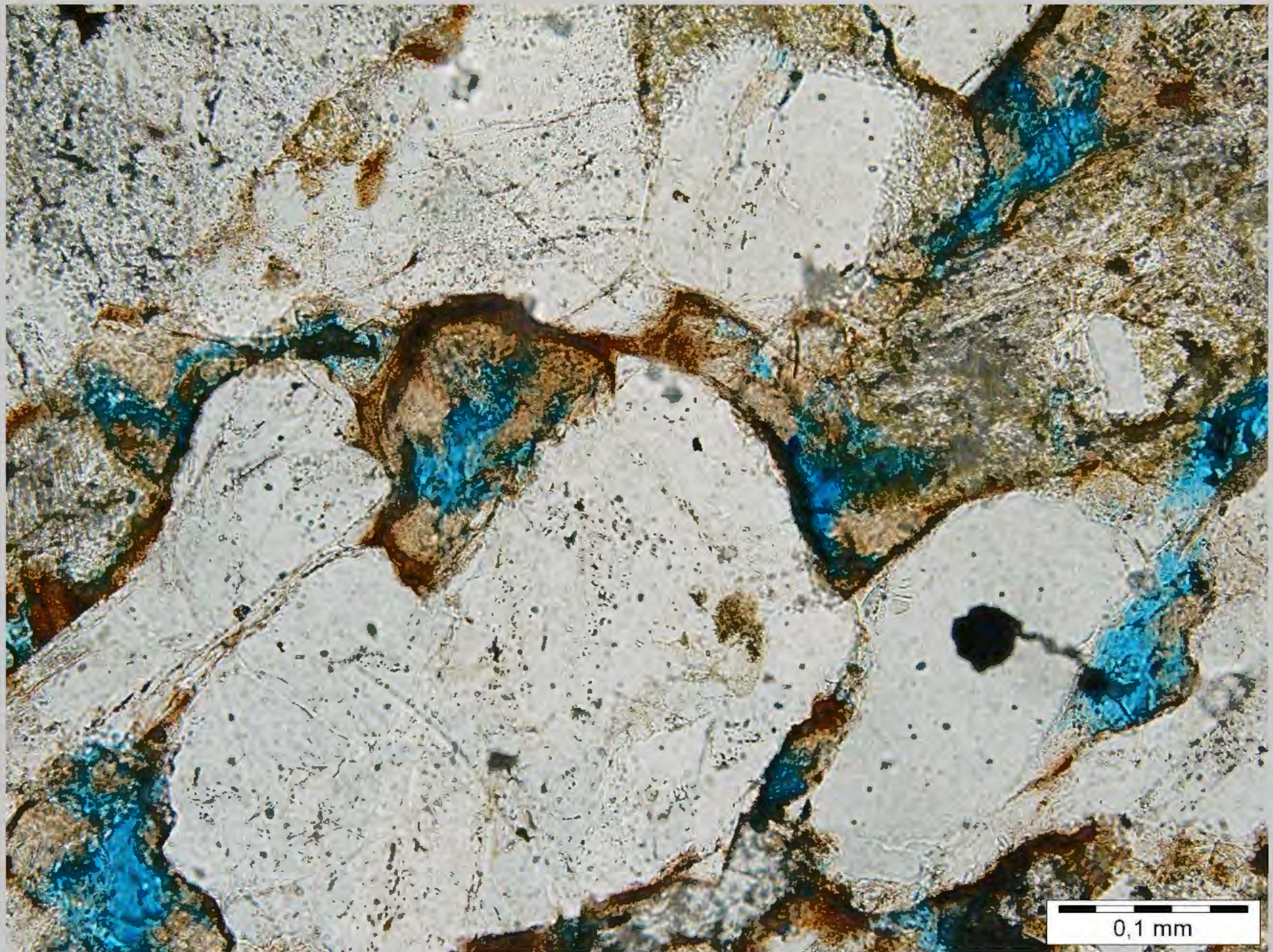
DATA USED TO DEFINE FLOW UNITS

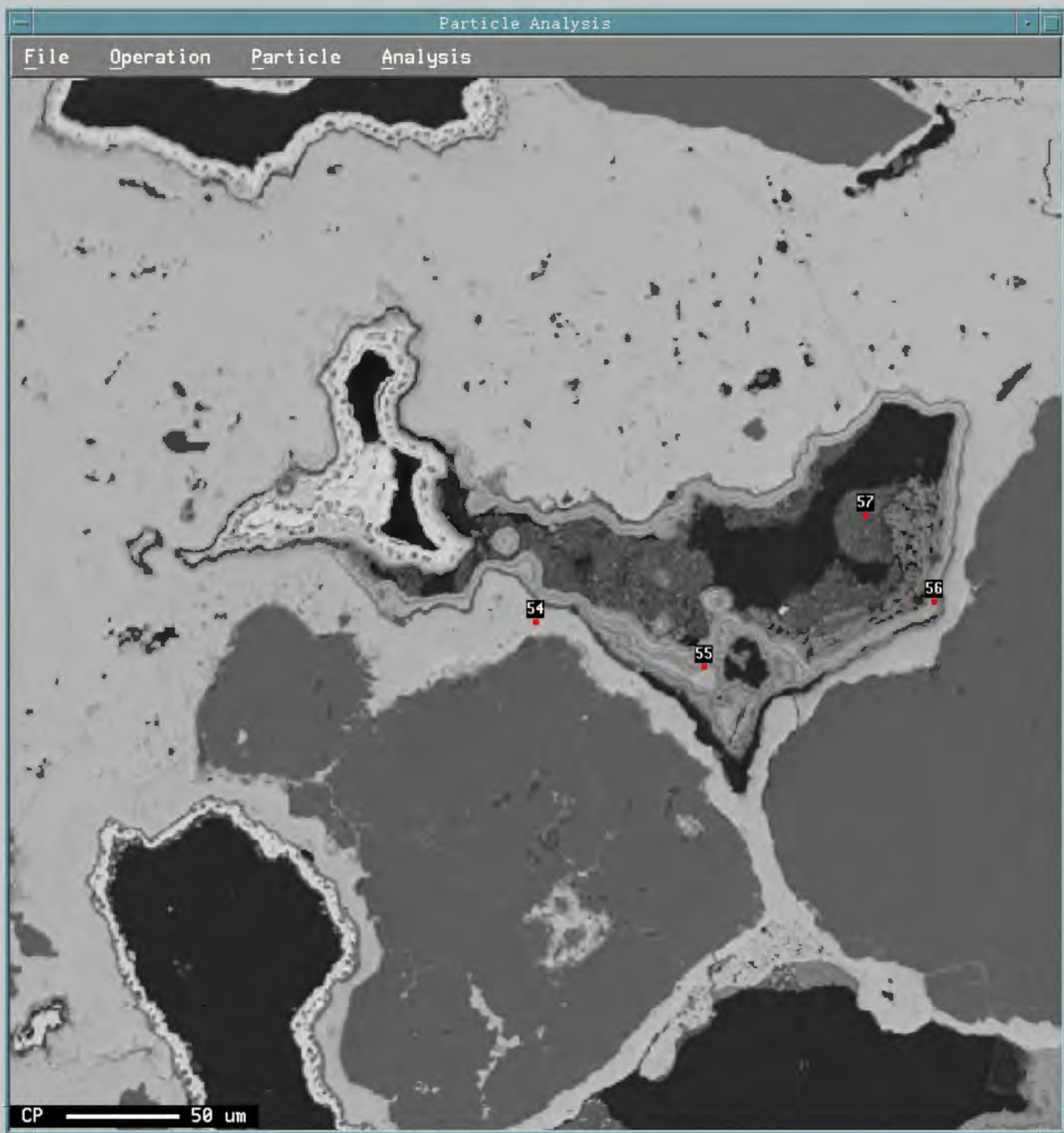


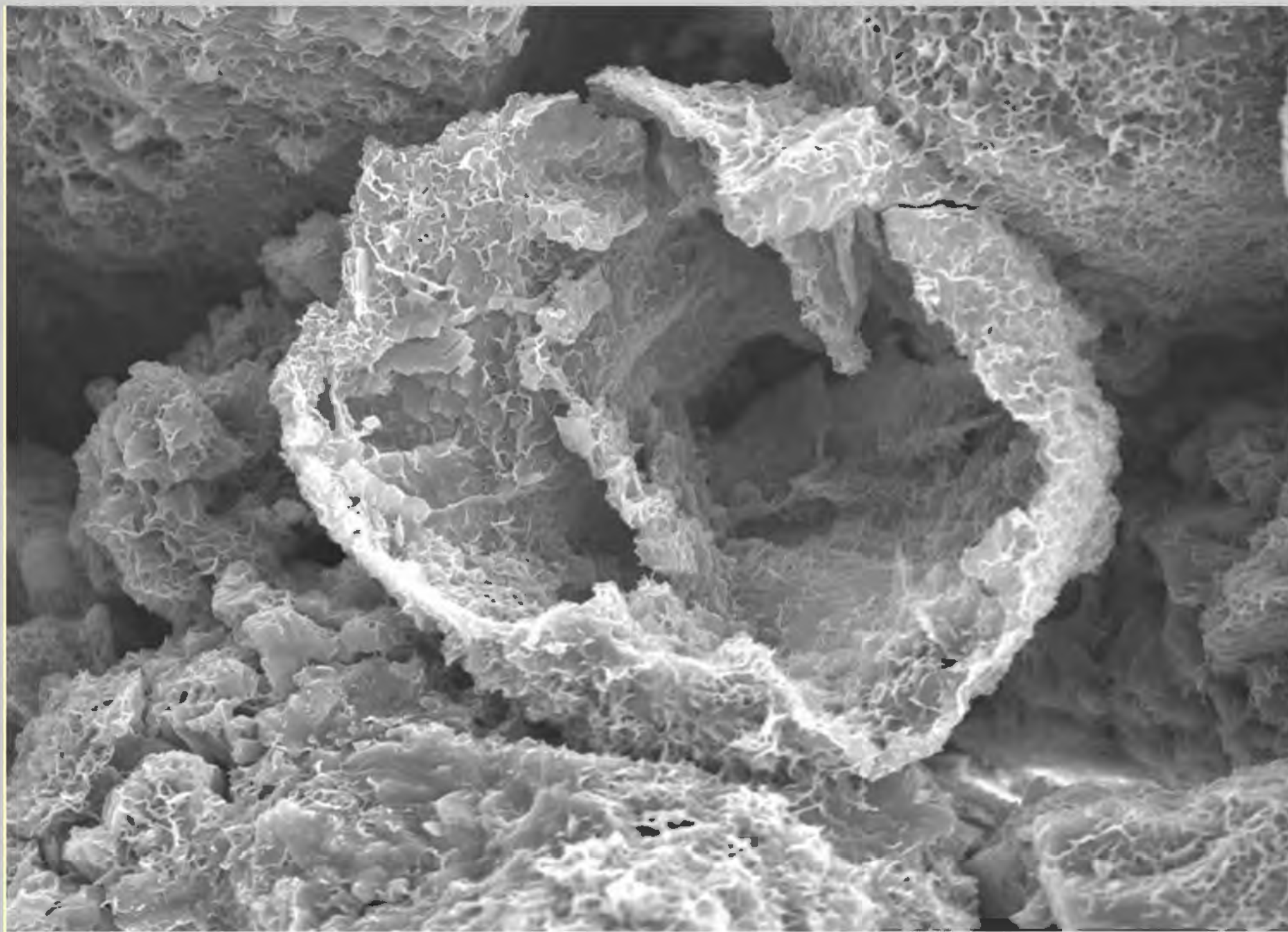
If your 1 foot section is heterolithic, where will the plug be taken from?

Modified from Ebanks et al. 1992, Fig 1, AAPG Dev. Geol. Ref. Manual.



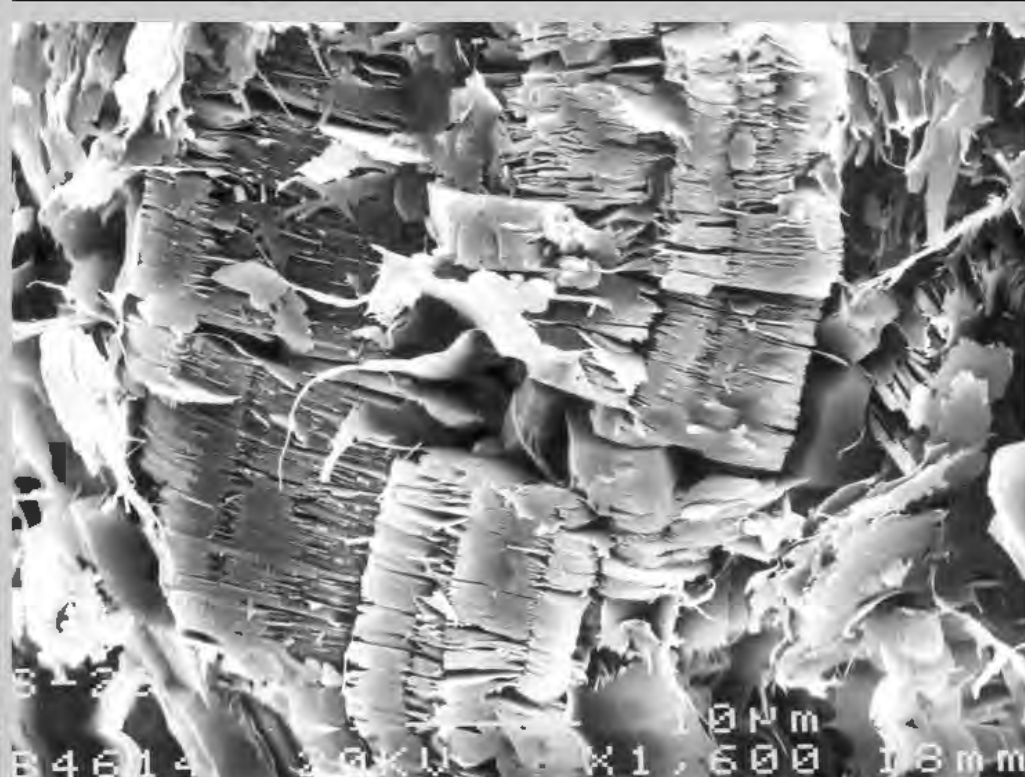
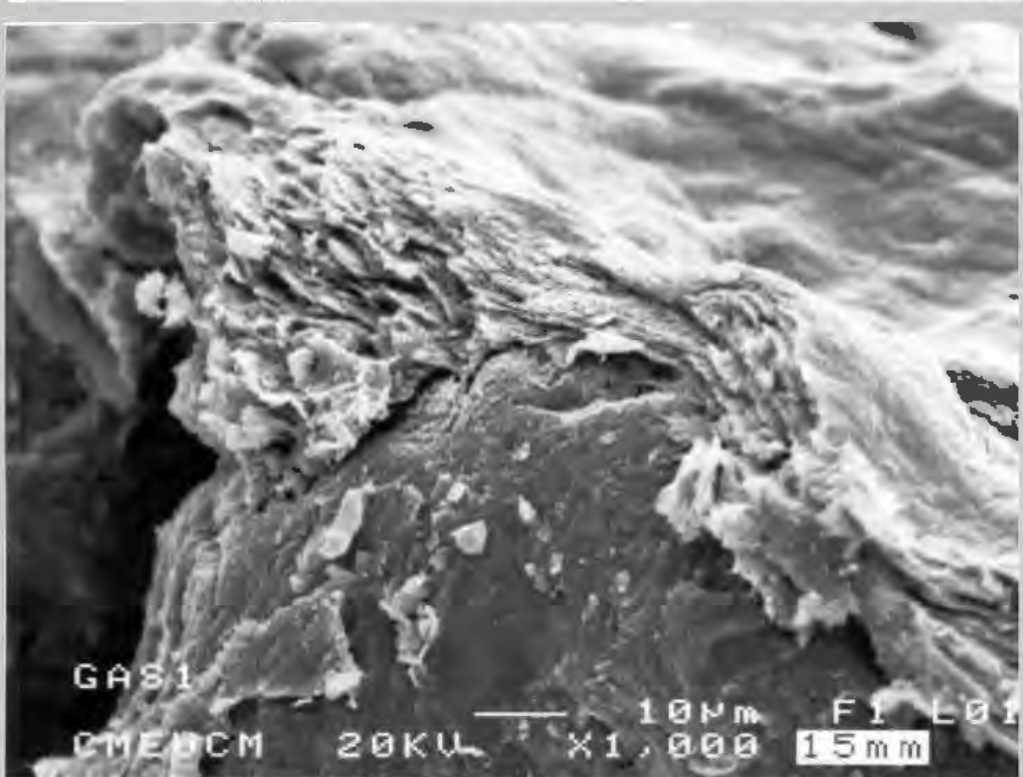
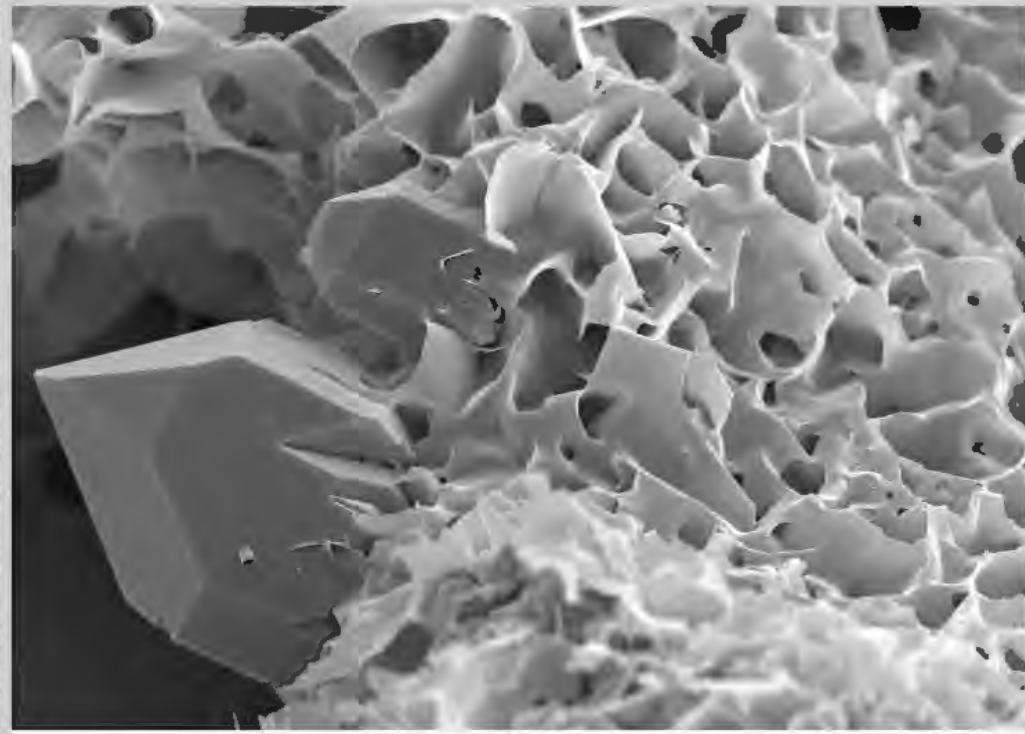
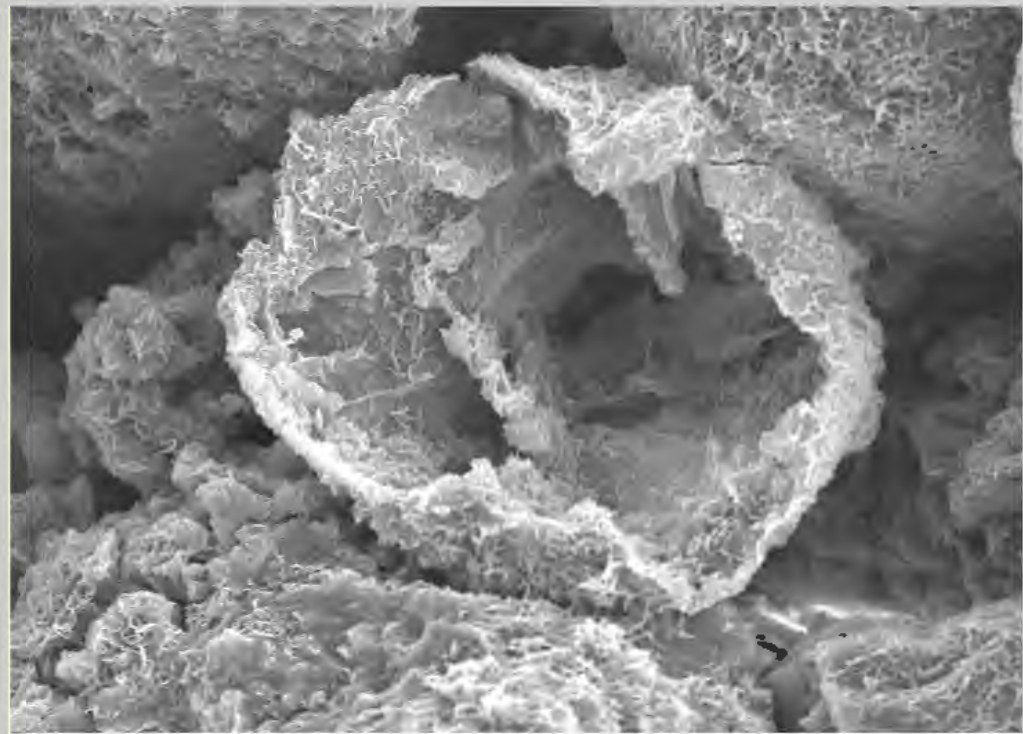






60 μ m

J. Arribas, 2010

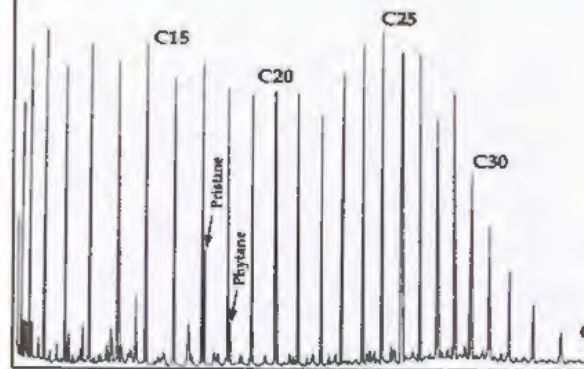


Similar to previous;

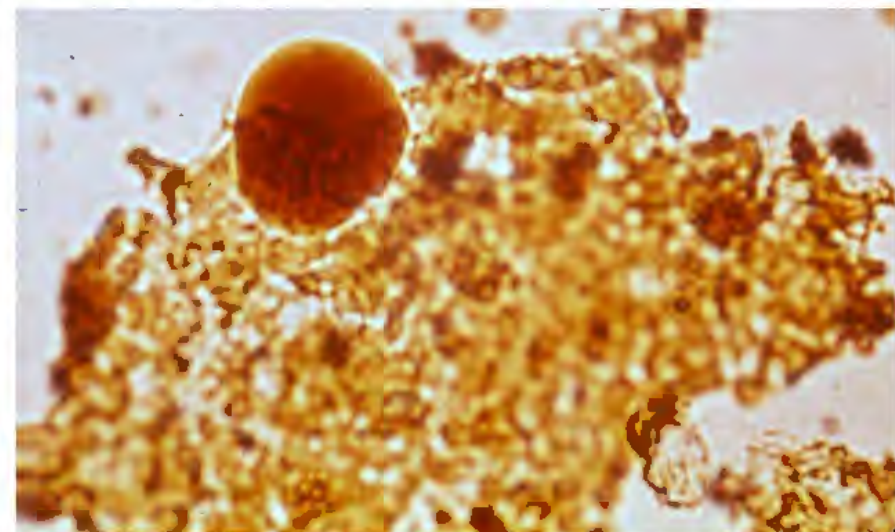


Fingerprinting of Hydrocarbons

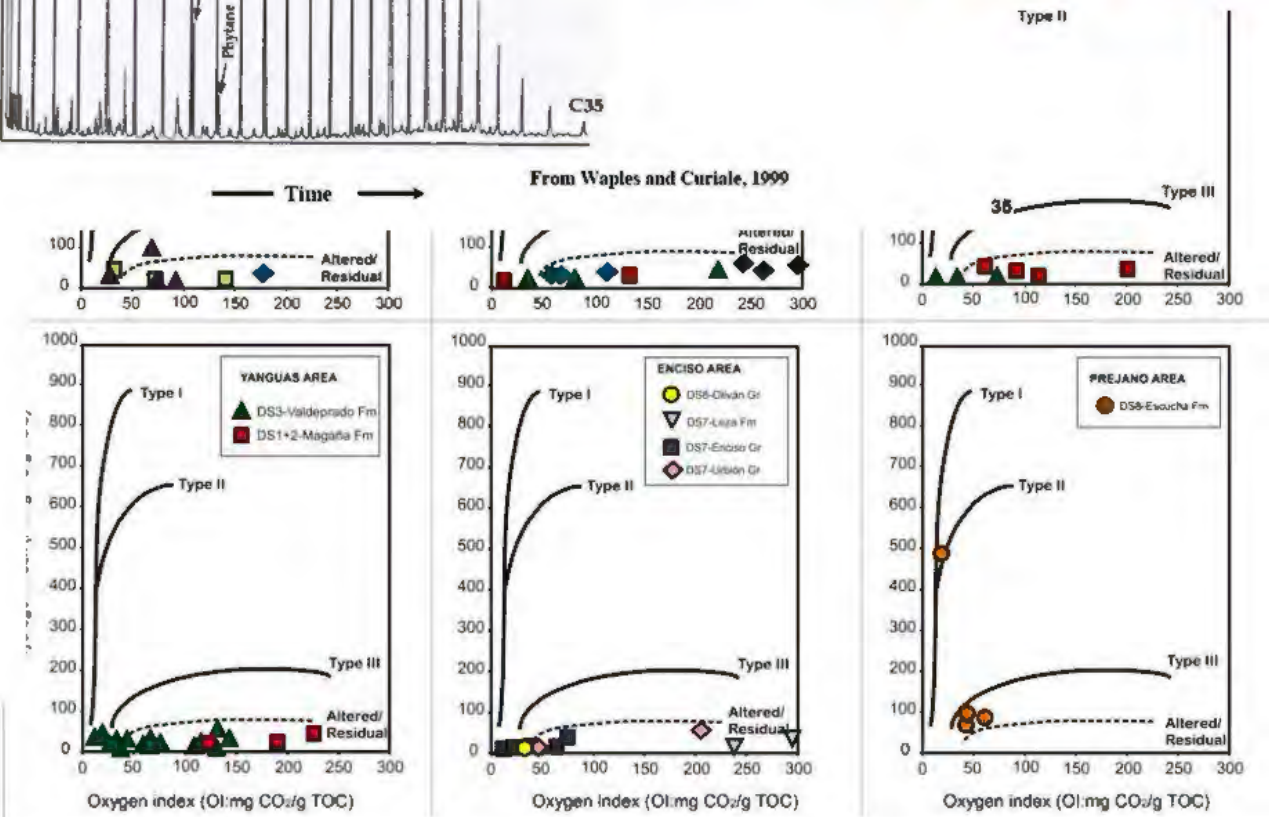
Gas Chromatography Used to Detect Abundance of Hydrocarbon Compounds



Chromatogram of high-wax oil of terrestrial origin



Momper, 1981, fig. 42

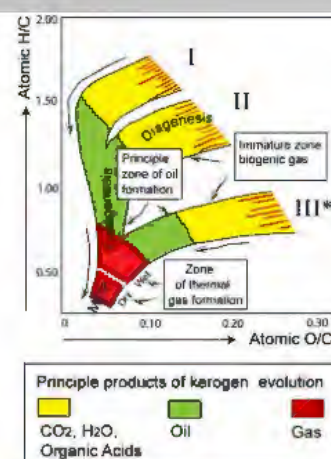
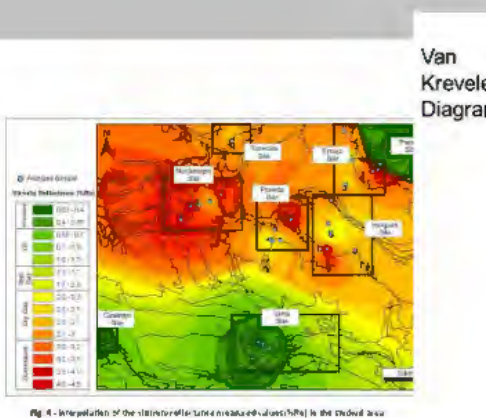
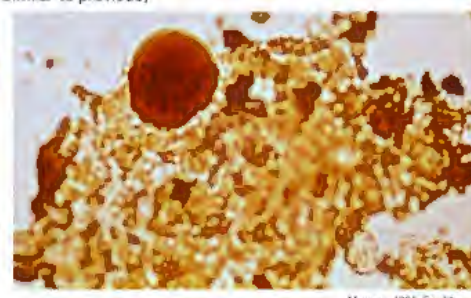




PRIMARY MIGRATION

Oil generation & expulsion from kerogen (Momper, 1981)

Similar to previous;



* Amount of oil generated by Type III is small

Fingerprinting of Hydrocarbons

Gas Chromatography Used to Detect Abundance of Hydrocarbon Compounds

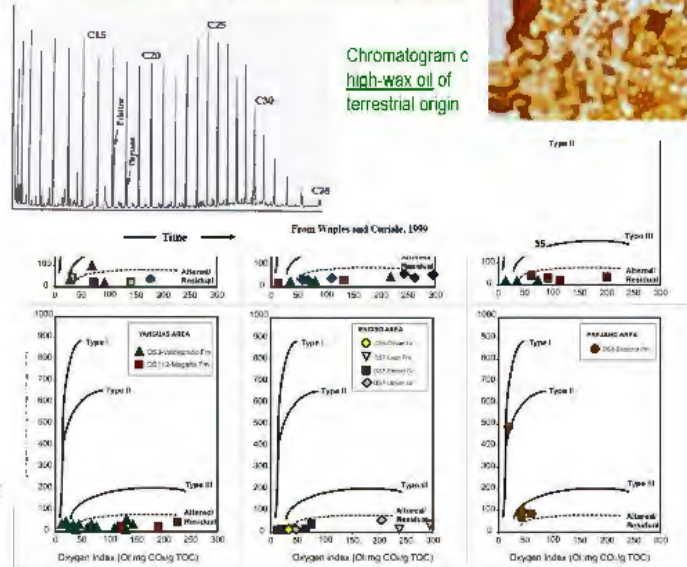
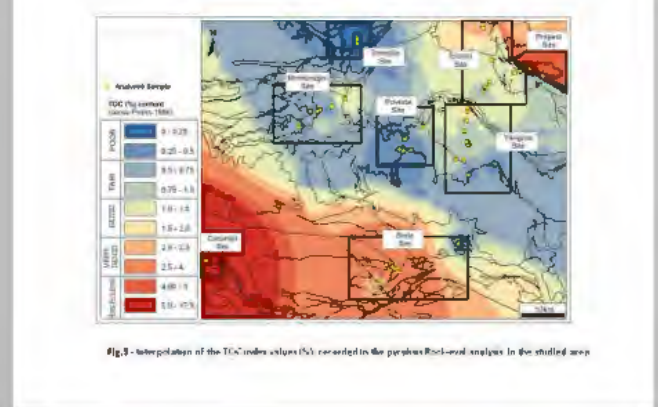
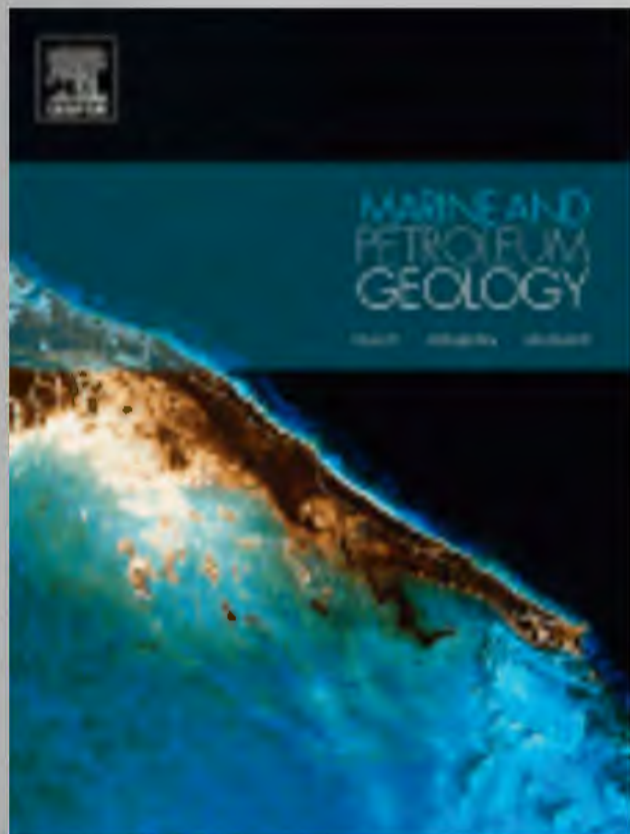


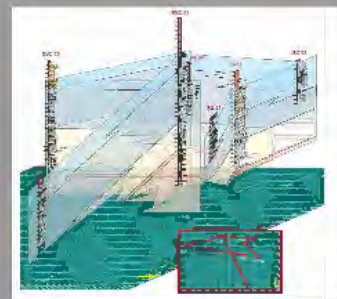
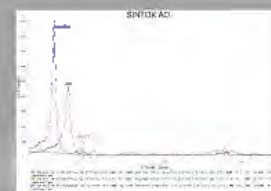
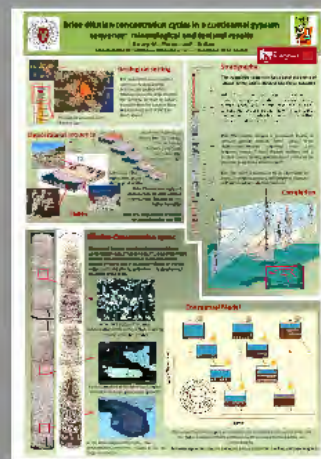
Fig.6-Hydrogen and oxygen index data plotted on a pseudo-Van Krevelen diagram (from Espitalie et al., 1986)

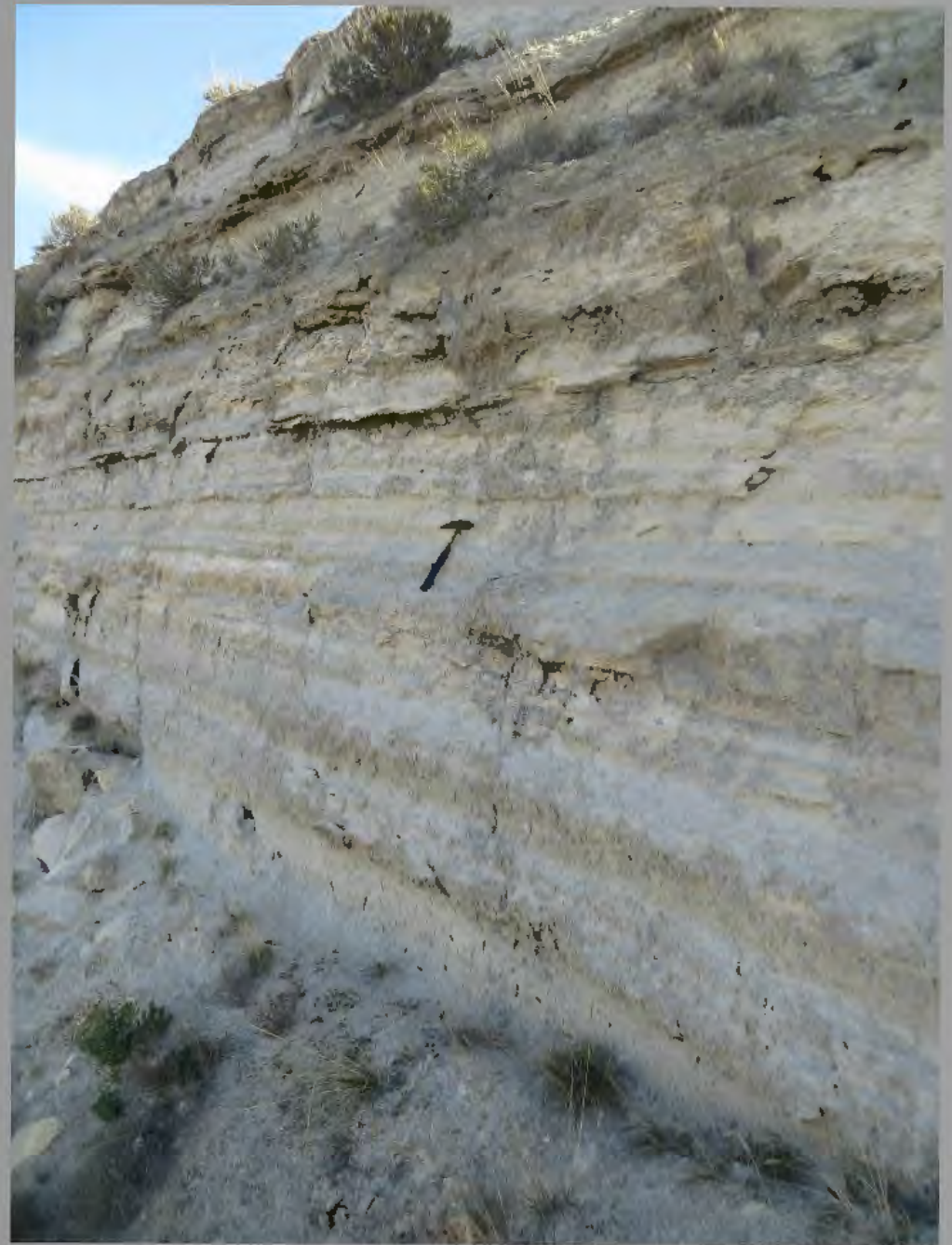




ATC

Almacén Temporal Centralizado de Residuos Nucleares





MESA SOMBREADA
TABA 91 995 42 74
TAB 91 995 42 12
SISTEMA PUEBLOMAYO DE 10 MM

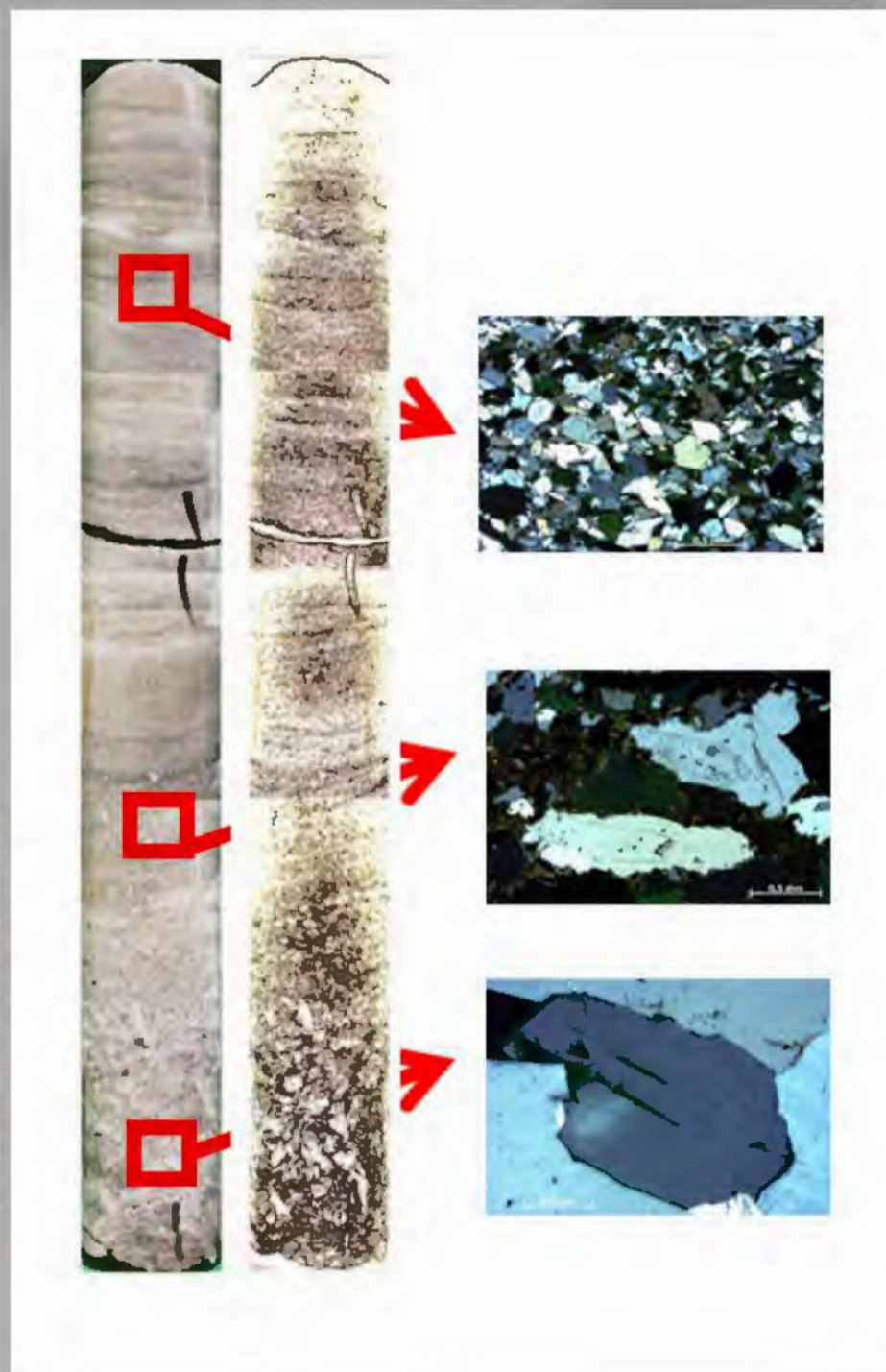
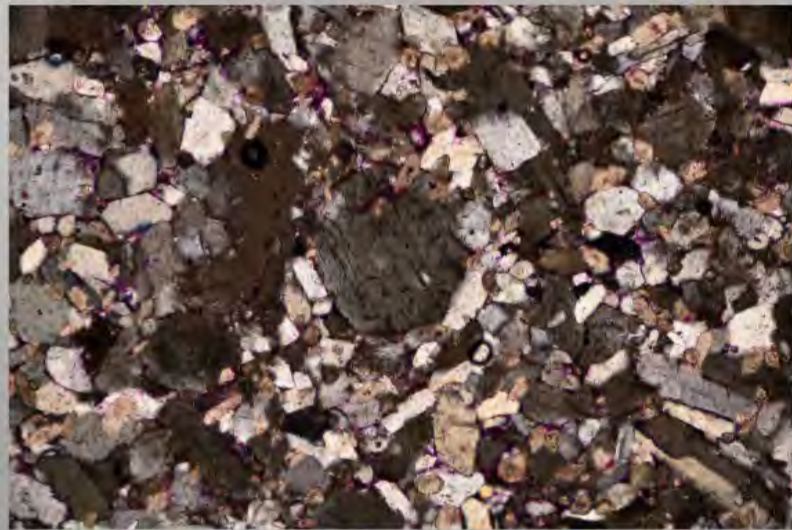
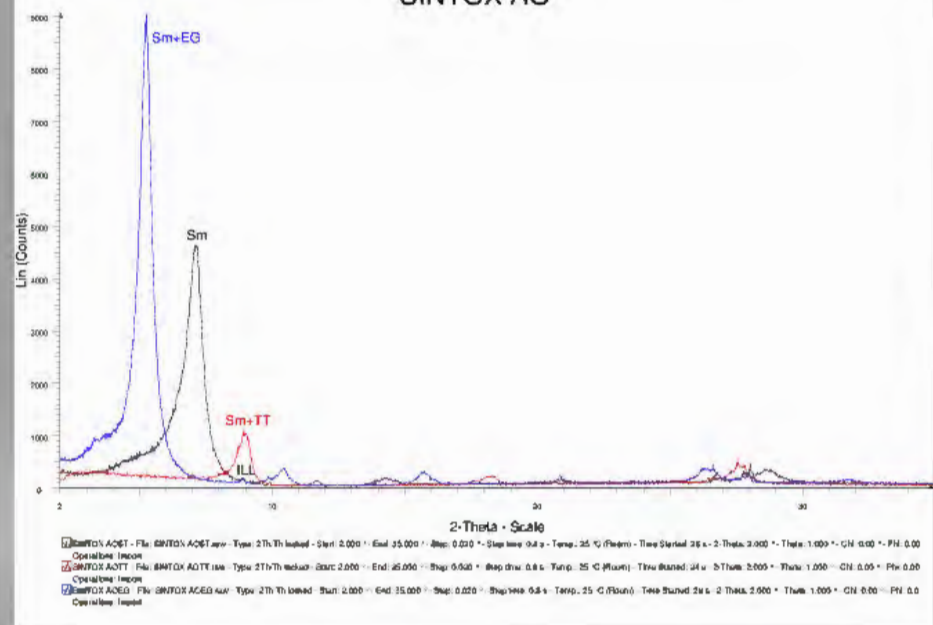
Profundidad de 3'00 Mts. A 6'00 Mts. Caja N° 12

3'00

6'00



SINTOX AO





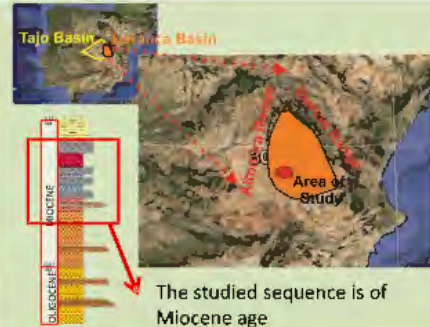
Brine dilution-concentration cycles in a continental gypsum sequence: mineralogical and textural results

J. Escavy, M.J. Herrero and J. Arribas

Departamento de Petrología y Geoquímica, Fac. CC. Geológicas, UCM, Madrid



IMS2015
KRAKOW, POLAND
22-25 JUNE 2015



Geological setting

The research herein presented concerns the depositional systems and cyclicity of the Miocene evaporite units found in the "Sinclinal de Villar de Cañas", located within the Loranca Basin (westernmost part of the Tajo Basin, Spain).

Depositional sequence



The oldest material are alluvial fans (T1, unit UI).

The alluvial fan retrogrades and forms marsh lacustrine environments (T2).

Saline lake (T3)
high salinity peaks during great aridity.

T4 to T5 formed by cycles of dilution-concentration within a perennial lake. Towards the top higher humidity.

Final new progradation of alluvial fan deposits in this area (T6)



Stratigraphy

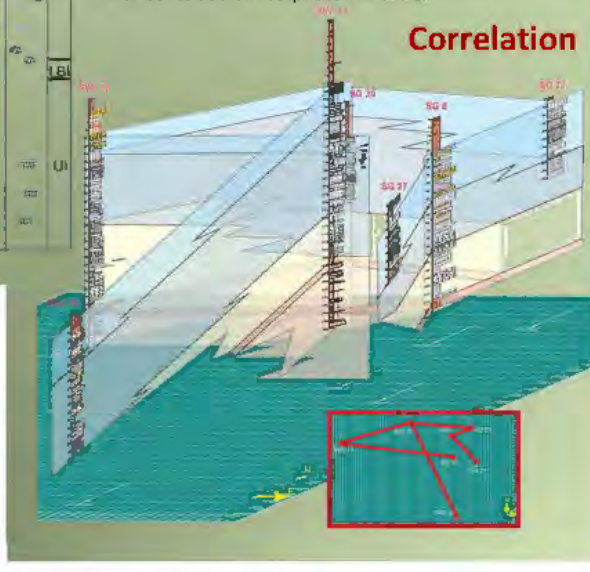
The evaporitic sequence has a total thickness of about 120 m and is divided into three subunits

YB3: The uppermost evaporitic subunit is characterized by an alternation of shale and primary gypsum beds, and in this case the dilution-concentration cycles start with the entrance into the basin of detrital materials transported by water that produced the dilution of the brine.

YB2: The second subunit is composed mainly of primary gypsum deposits where several brine dilution-concentration sequences occur. Each sequence reveals a basal dilution surface and a marked crystal finning upwards trend produced by the brine progressive concentration.

YB1: The lower is composed by an alternation of shales, secondary gypsum, and anhydrite deposits with some sodium sulphate minerals.

Correlation



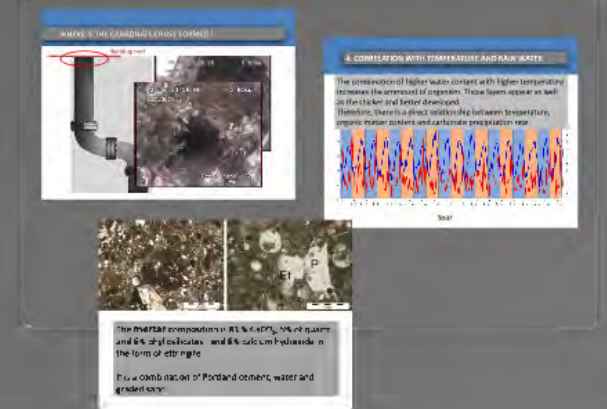
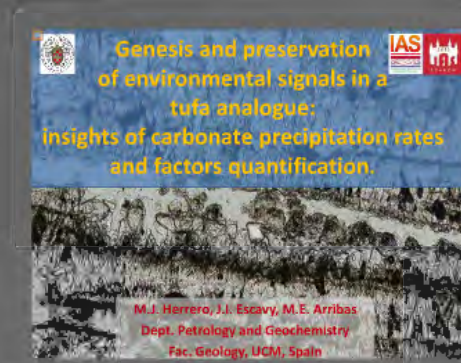
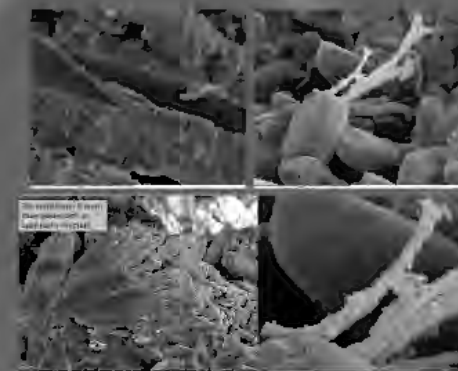
Dilution-Concentration cycles

The textural features permit to characterize dilution-concentration cycles that compose the evaporitic middle subunit. The characterization of these cycles in the geological record appear as a good indicator of shallow water depth and climate control over the geochemical character of the brine.

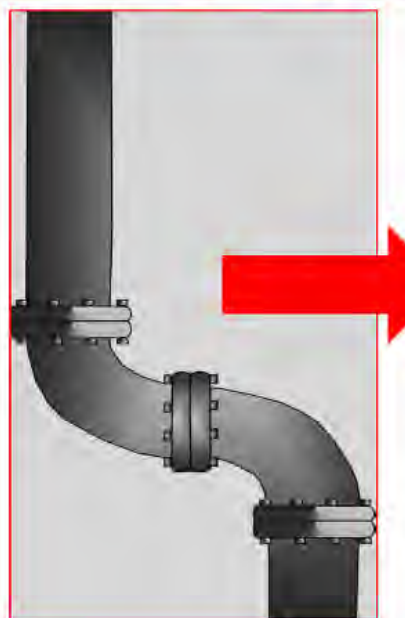


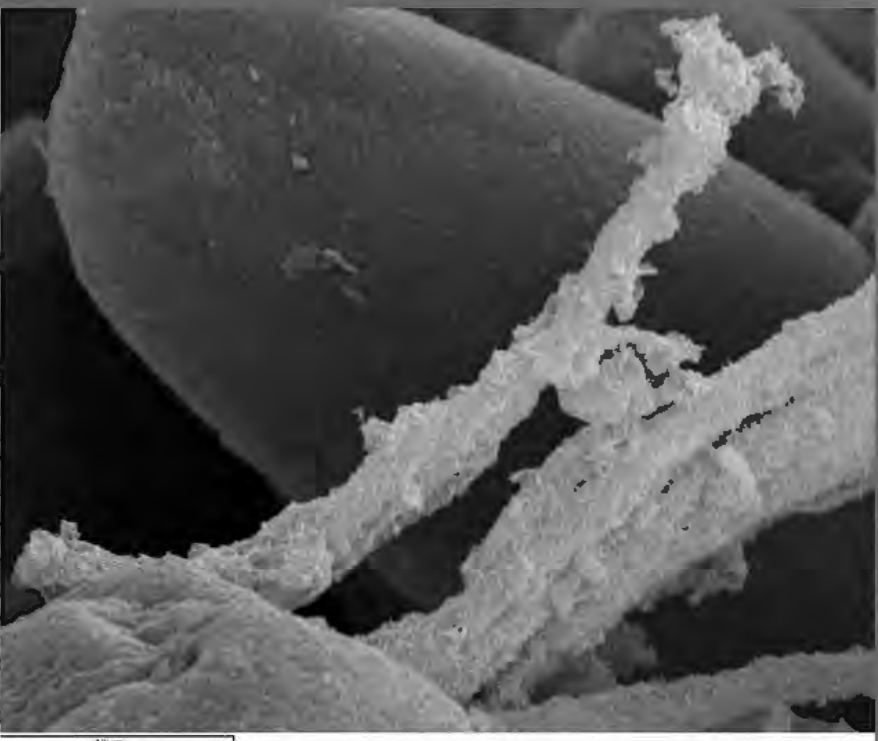
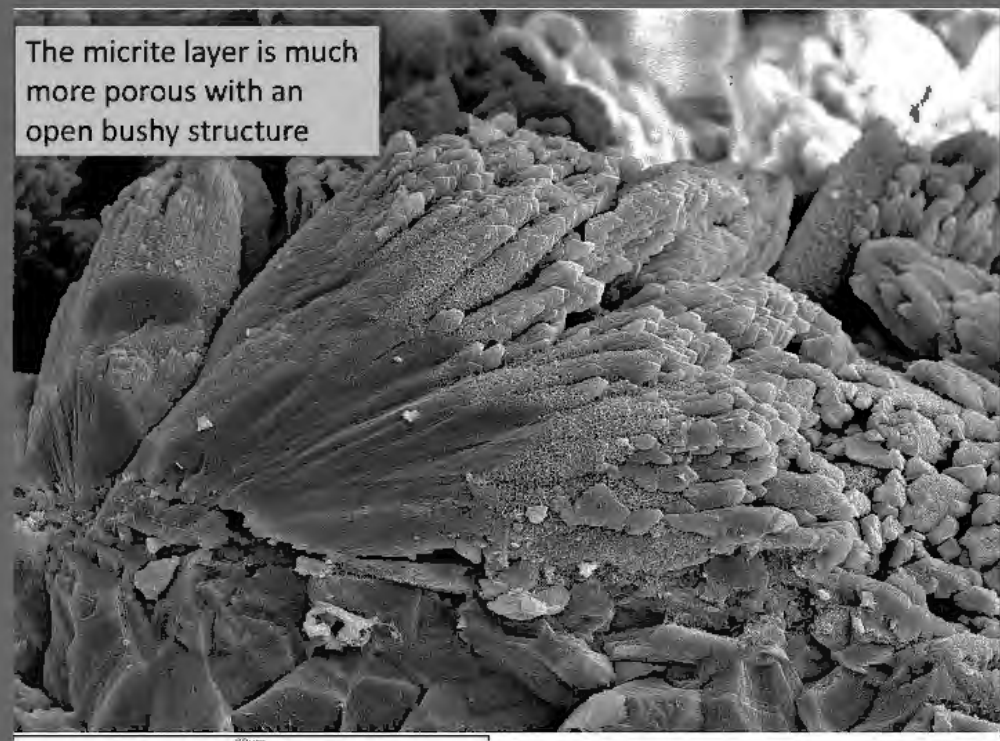
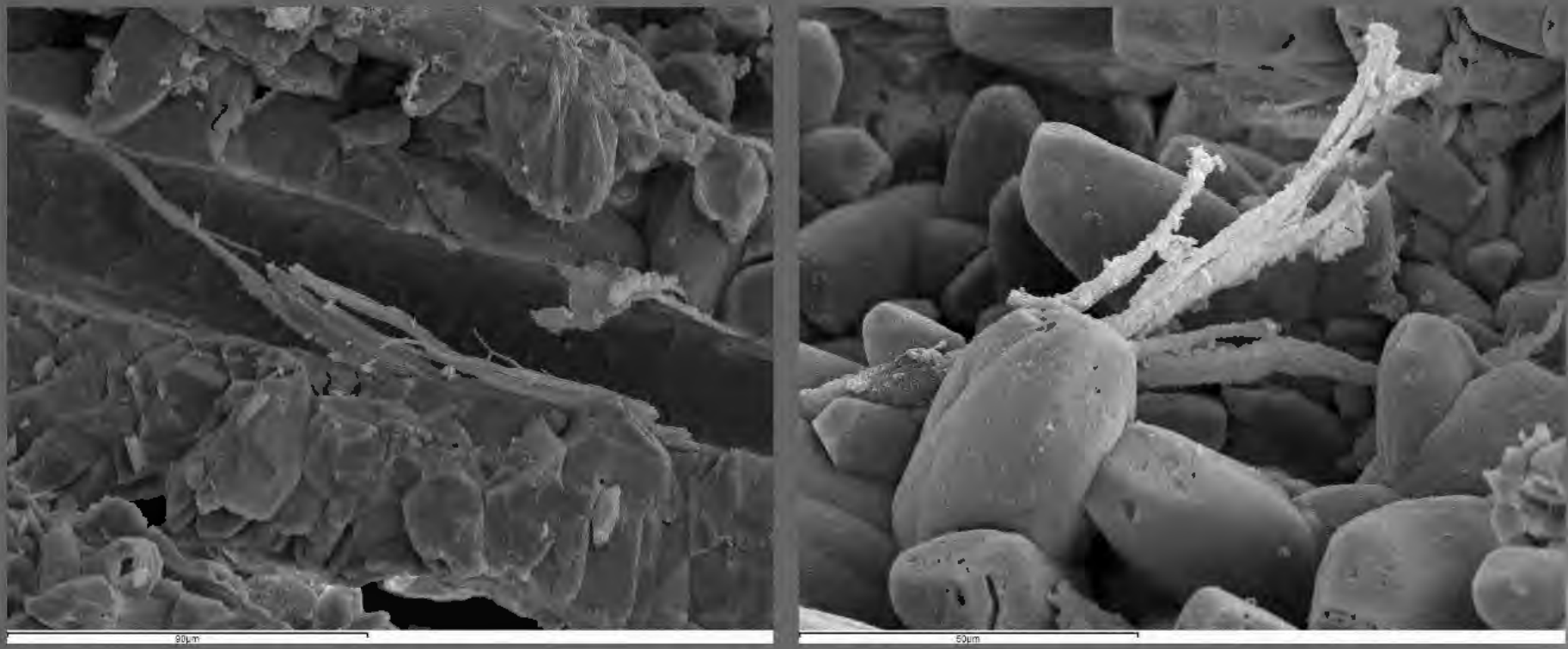
Conceptual Model

Concreciones en edificio de San Sebastian



LOCATION OF THE STUDY SITE



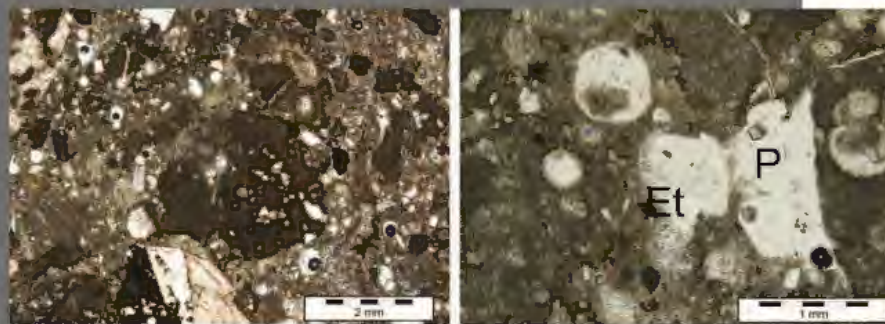
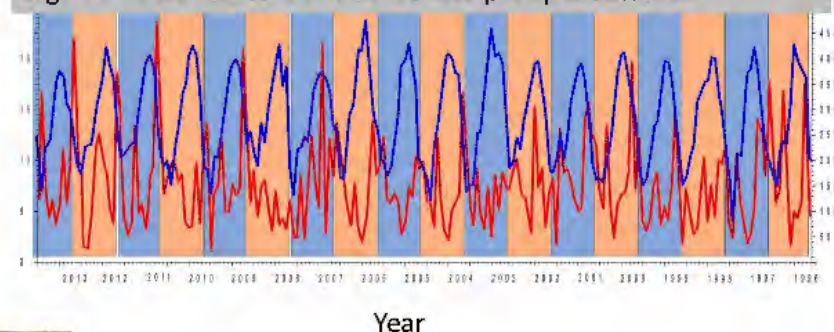


WHERE IS THE CARBONATE CRUST FORMED?



4. CORRELATION WITH TEMPERATURE AND RAIN WATER

The combination of higher water content with higher temperature increases the amount of organism. Those layers appear as well as the thicker and better developed. Therefore, there is a direct relationship between temperature, organic matter content and carbonate precipitation rate

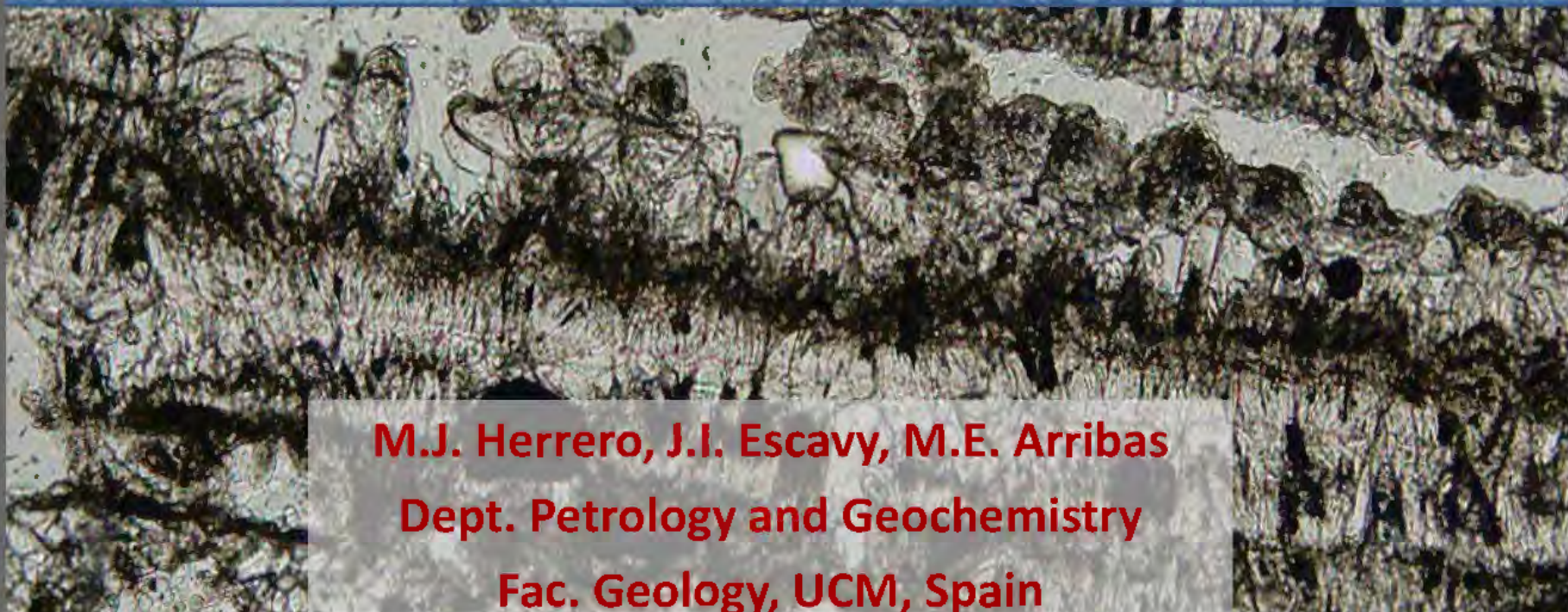


The **mortar** composition is 83 % CaCO_3 , 5% of quartz and 6% phyllosilicates, and 6% calcium hydroxide in the form of ettringite

It is a combination of Portland cement, water and graded sand

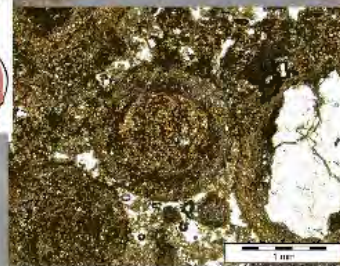


Genesis and preservation of environmental signals in a tufa analogue: insights of carbonate precipitation rates and factors quantification.



M.J. Herrero, J.I. Escavy, M.E. Arribas
Dept. Petrology and Geochemistry
Fac. Geology, UCM, Spain

Análisis de Actividad de Fallas



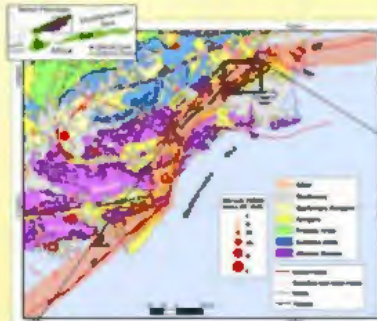
B448. UPPER PLEISTOCENE - HOLOCENE ACTIVITY OF THE CARRASCOY FAULT (MURCIA, SE SPAIN): PRELIMINARY RESULTS FROM PALEOSEISMOLOGICAL RESEARCH



Martín-Banda, R.¹, García-Mayordomo, J.², Insua-Arévalo, J.M.¹, Salazar, A.², Rodríguez-Escudero, E.³, Álvarez-Gómez, J.A.¹, Martínez-Díaz, J.J.¹, Herrero, M.J.⁴, Mediadeas, A.⁵

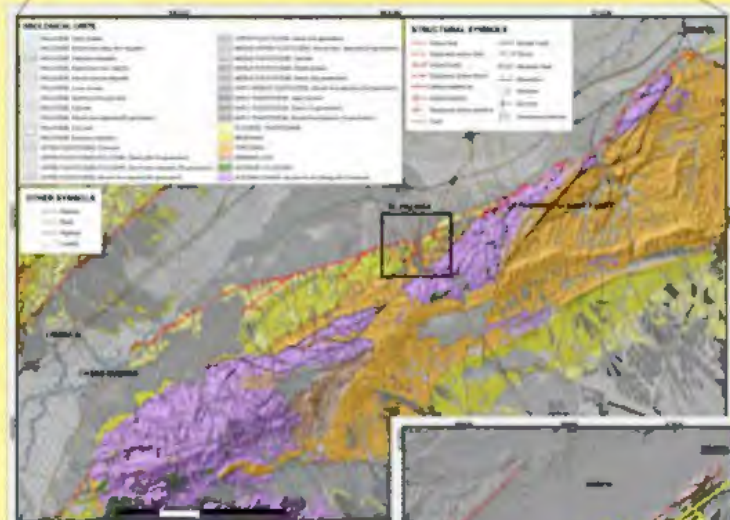
¹-Dept. of Geodynamics, Complutense University of Madrid, Spain. rsmartin0@ucm.es; insuaar@geo.ucm.es; jmlazaro@geo.ucm.es; jmdiaz@geo.ucm.es. ²- Spanish Geological Survey (IGME), Madrid, Spain. julian.garcia@igme.es; a.salazar@igme.es. ³- Dept. of Geology and Geochemistry, Autónome University of Madrid, Spain. emilio.rodriguez@uam.es. ⁴- Dept. of Petrology, Complutense University of Madrid, Spain. mherrero@ucm.es. ⁵- Dept. of Geography, University of Sheffield, UK. a.mediadeas@shef.ac.uk

FAULT TRACE MAPPING



The Carrascoy Fault (CAF) is located in the Internal Zones of the Betic Cordillera (Southern Spain). It is one of the main faults forming the Eastern Seismic Zone (ESZ), a major structure accommodating the convergence between African and European plates of the westernmost part of the Mediterranean sea (Luisa et al., 1998; Olivé et al., 1993).

So far, the CAF has been defined as a left-lateral active fault (Herrera, 1994; Sanz de Galdeano et al., 1995). It trends NE-SW, controlling the northern front of the Carrascoy Range and, towards the west, the margin of the Guadalest Depression. This is an area of moderate seismic activity, but rarely published, the Murcia city being within easy access to the fault, hence, the knowledge of the structure and kinematics of the CAF is essential for a reliable assessment of the seismic hazard of the region.

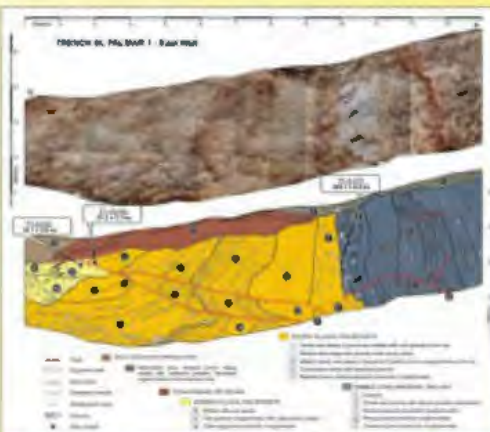


NEW SEGMENTATION OF CAF

According to our studies, the fault can be divided into two overlapping segments: the western one, CASAS NUEVAS - FUENSANTA (CN-F), and the eastern one, EL PALMAR - ZEQUETA (EP-Z). The delineation of the CN-F segment clearly splits it into two strands, North-Carrascoy (forming the northern border of the main relief) and a new formed strand located seawards. This new strand shows a clear zone related fault motion with associated folding.

PALEOSEISMIC STUDY OF CN-F SEGMENT

Palmar-1 and Palmar-2 are the names of two trenches dug across the CN-F segment. Palmar-1 trench intersected the fault, showing its reverse kinematics. At level one paleoseismological event was identified. The most recent deposits affected by the fault have been dated by Optically Stimulated Luminescence (OSL).



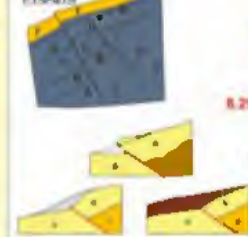
On the contrary, no deformation was observed in the younger deposits excavated in the Palmar-2 trench. These deposits were dated by radiocarbon as well as C-14 at 6200 ± 300 years postdating the last seismic event.



CONCLUSIONS

North Carrascoy System

$>209.1 \pm 6.2$ ka
P1-3-UTH

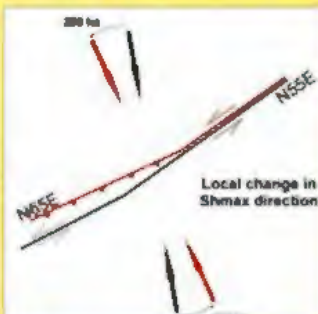


Casas Nuevas - Fuentanya System

$>209.1 \pm 6.2$ ka



8.29 ± 0.04 ka < seismic < 14.1 ± 2.5 ka event



Local change in Shmax direction

3. A local change in the maximum horizontal shortening direction that occurs from NW-SE to NW-NE, the latter being responsible for the sinistral strike-slip kinematics since Upper Tertiary and the former for an increase in the reverse component of the fault movement from Middle-Upper Pleistocene times.

4. The paleoseismological study suggests that a change in Shmax occurred about 200 ka (upper part of the Middle Pleistocene), and that the last perfect rupture event took place between 14.1 and 8.2 ka.

REFERENCES

- Luisa, S.C., Briceño, J.J., Gutiérrez, D., Elizalde, C., 2004. Paleogeography of the Iberian Peninsula during the Middle Miocene. *Tectonophysics* 432, 103–120.
- Oliver, J., 1993. Geodynamic evolution of the Iberian Peninsula. In: García-Palomo, A., Martínez-Díaz, J.J. (Eds.), *Geodynamics of the Iberian Peninsula*. Elsevier, Amsterdam, pp. 13–40.
- Olivé, A., 1993. Geodynamic evolution of the Iberian Peninsula. In: García-Palomo, A., Martínez-Díaz, J.J. (Eds.), *Geodynamics of the Iberian Peninsula*. Elsevier, Amsterdam, pp. 13–40.
- Sanz de Galdeano, J., 1994. Luminiscencia óptica en depósitos terciarios y cuaternarios del sistema Cárabo-Carrascoy. *Revista de la Unión Geológica de España* 105, 295–303.



Pleistocene calcrete deposits from southern Spain as indicators of climatic conditions and tectonic activity



Instituto Geológico
y Minero de España

Maria J. Herrero (1), Juan M. Insua-Arevalo (2), Julian Garcia-Mayordomo (3), Raquel Martin-Banda (2)

(1) DPT. PETROLOGIA Y GEOQUIMICA (UCM); (2) DEPT. GEODINAMICA (UCM); (3) INSTITUTO GEOLOGICO Y MINERO (IGME)

1. INTRODUCTION



The Quaternary sediments of the study area have been interpreted as being deposited during the last glacial period, with the Quaternary Period.

It is widely accepted that the Quaternary sediments are formed by glaciogenic processes, particularly in mountainous regions such as the Pyrenees. The former surfaces are covered by talus slopes with glaciogenic material derived from the high altitude, whereas the lower slopes are covered by glaciogenic material.

2. GEOLOGICAL SETTING



3. OUTCROP ANALYSIS

Chlorite development

Chlorite development is observed in different facies, mainly chlorite.

Chlorite with intergrown quartz in Fig. 3A, with weathering in the following stages:

Initially, the chlorite is chloritized. The chlorite weathering produces chlorite and finally forms a chlorite-chlorite-talc.

Chlorite with talc with chlorite and talc in Fig. 3B, with weathering in the following stages:

Chlorite with talc with chlorite and talc in Fig. 3C, with weathering in the following stages:

Chlorite with talc with chlorite and talc in Fig. 3D, with weathering in the following stages:

Chlorite with talc with chlorite and talc in Fig. 3E, with weathering in the following stages:

Chlorite with talc with chlorite and talc in Fig. 3F, with weathering in the following stages:

Chlorite with talc with chlorite and talc in Fig. 3G, with weathering in the following stages:

Chlorite with talc with chlorite and talc in Fig. 3H, with weathering in the following stages:

Chlorite with talc with chlorite and talc in Fig. 3I, with weathering in the following stages:

Chlorite with talc with chlorite and talc in Fig. 3J, with weathering in the following stages:

Chlorite with talc with chlorite and talc in Fig. 3K, with weathering in the following stages:

Chlorite with talc with chlorite and talc in Fig. 3L, with weathering in the following stages:

Chlorite with talc with chlorite and talc in Fig. 3M, with weathering in the following stages:

Chlorite with talc with chlorite and talc in Fig. 3N, with weathering in the following stages:

4. PETROLOGY AND XRD ANALYSES

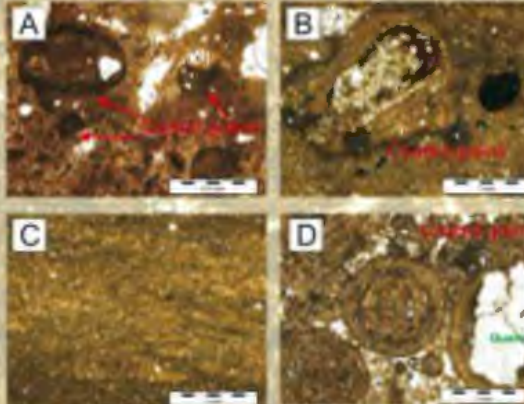


Figure 4. Different calcrete structures observed in the study area. A: Layered calcrete; B: Encrusting calcrete; C: Lenticular calcrete; D: Vuggy calcrete.

At the bottom right of Fig. 4, the age of the calcrete deposit has been estimated by thermometric methods, using U-Th dating, a single whole-rock analysis of the normal profile of the field.

The bottom right of Fig. 4, the age of the calcrete deposit has been estimated by thermometric methods, using U-Th dating, a single whole-rock analysis of the normal profile of the field.

The bottom right of Fig. 4, the age of the calcrete deposit has been estimated by thermometric methods, using U-Th dating, a single whole-rock analysis of the normal profile of the field.

The bottom right of Fig. 4, the age of the calcrete deposit has been estimated by thermometric methods, using U-Th dating, a single whole-rock analysis of the normal profile of the field.

The bottom right of Fig. 4, the age of the calcrete deposit has been estimated by thermometric methods, using U-Th dating, a single whole-rock analysis of the normal profile of the field.

The bottom right of Fig. 4, the age of the calcrete deposit has been estimated by thermometric methods, using U-Th dating, a single whole-rock analysis of the normal profile of the field.

The bottom right of Fig. 4, the age of the calcrete deposit has been estimated by thermometric methods, using U-Th dating, a single whole-rock analysis of the normal profile of the field.

The bottom right of Fig. 4, the age of the calcrete deposit has been estimated by thermometric methods, using U-Th dating, a single whole-rock analysis of the normal profile of the field.

The bottom right of Fig. 4, the age of the calcrete deposit has been estimated by thermometric methods, using U-Th dating, a single whole-rock analysis of the normal profile of the field.

The bottom right of Fig. 4, the age of the calcrete deposit has been estimated by thermometric methods, using U-Th dating, a single whole-rock analysis of the normal profile of the field.

The bottom right of Fig. 4, the age of the calcrete deposit has been estimated by thermometric methods, using U-Th dating, a single whole-rock analysis of the normal profile of the field.

The bottom right of Fig. 4, the age of the calcrete deposit has been estimated by thermometric methods, using U-Th dating, a single whole-rock analysis of the normal profile of the field.

The bottom right of Fig. 4, the age of the calcrete deposit has been estimated by thermometric methods, using U-Th dating, a single whole-rock analysis of the normal profile of the field.

The bottom right of Fig. 4, the age of the calcrete deposit has been estimated by thermometric methods, using U-Th dating, a single whole-rock analysis of the normal profile of the field.

The bottom right of Fig. 4, the age of the calcrete deposit has been estimated by thermometric methods, using U-Th dating, a single whole-rock analysis of the normal profile of the field.

The bottom right of Fig. 4, the age of the calcrete deposit has been estimated by thermometric methods, using U-Th dating, a single whole-rock analysis of the normal profile of the field.

5. GEOCHRONOLOGY



By using thermometric U-Th dating methods are have obtained an age of formation of the limestone deposit (Table 1) of 209 ± 1.8 ka, part of the Undina Placer.

This age corresponds to the warm stage 11 within the glacial stage 11p. As pointed out before, the warm climate appears to reflect as a result of the activity of the Calcareous Fault.

Thanks to Fig. 4 we can see that the fault was reactivated only after the limestone was formed.

6. CONCLUSION

During the last century of the last glacial period, the limestone deposit formed by the dissolution of the limestone profile before any fault activity. This was due to the tectonic and climatic factors.

The calcrete formation and the limestone deposit are the result of the dissolution of the limestone profile before any fault activity.

During the last century of the last glacial period, the limestone deposit formed by the dissolution of the limestone profile before any fault activity.

The age of the limestone deposit has been estimated by thermometric methods, using U-Th dating.

The limestone deposit has been estimated by thermometric methods, using U-Th dating.

The limestone deposit has been estimated by thermometric methods, using U-Th dating.

The limestone deposit has been estimated by thermometric methods, using U-Th dating.

The limestone deposit has been estimated by thermometric methods, using U-Th dating.

The limestone deposit has been estimated by thermometric methods, using U-Th dating.

The limestone deposit has been estimated by thermometric methods, using U-Th dating.

The limestone deposit has been estimated by thermometric methods, using U-Th dating.

The limestone deposit has been estimated by thermometric methods, using U-Th dating.

The limestone deposit has been estimated by thermometric methods, using U-Th dating.

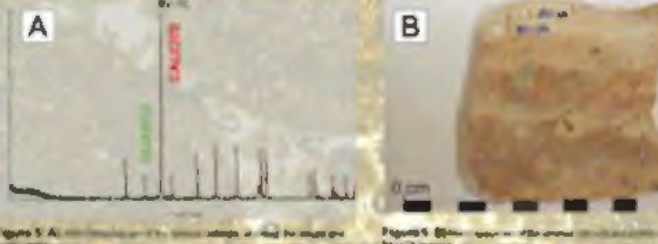


Figure 5. A: A vertical column of calcrete layers. B: A close-up view of a calcrete layer.

BIBLIOGRAPHY

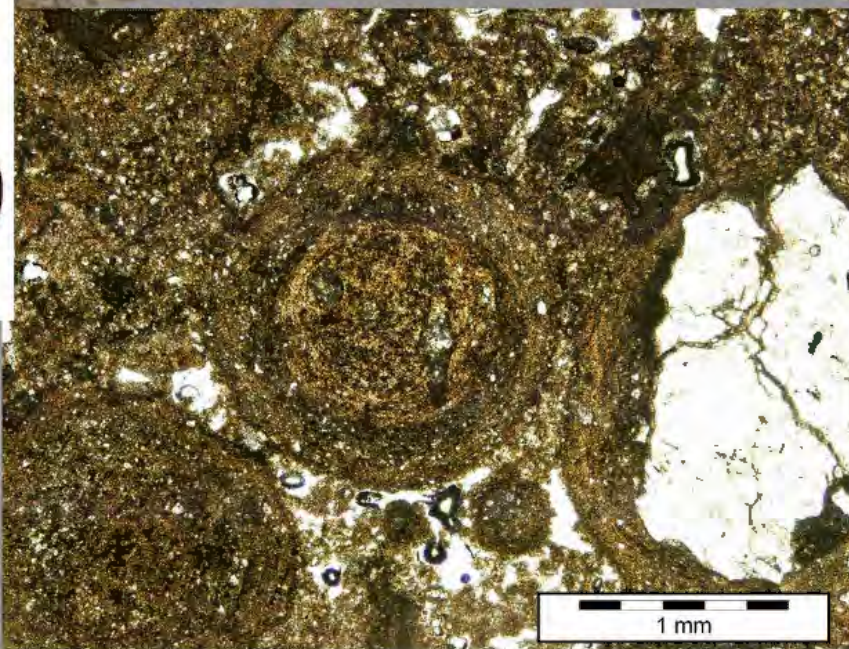
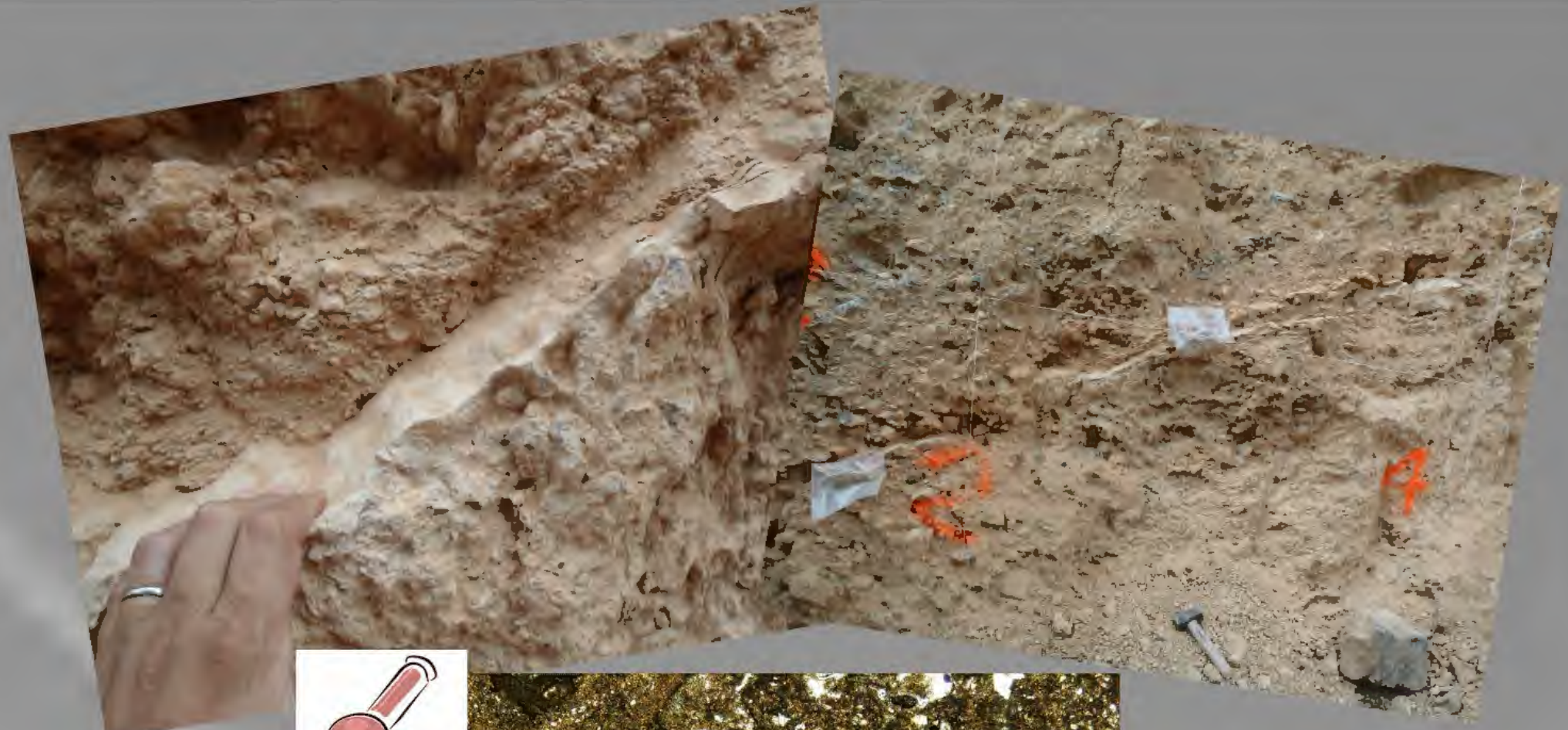
- Garcia-Mayordomo, J., Herrero, M.J., Insua-Arevalo, J.M., 2010. Tectonic and climatic control on the dissolution of limestone profiles in the Sierra Morena (Southern Iberia). *Geodinamica Acta* 23, 1–12.
- Herrero, M.J., Insua-Arevalo, J.M., Garcia-Mayordomo, J., 2009. Tectonic and climatic control on the dissolution of limestone profiles in the Sierra Morena (Southern Iberia). *Geodinamica Acta* 22, 1–12.
- Herrero, M.J., Insua-Arevalo, J.M., Garcia-Mayordomo, J., 2008. Tectonic and climatic control on the dissolution of limestone profiles in the Sierra Morena (Southern Iberia). *Geodinamica Acta* 21, 1–12.
- Herrero, M.J., Insua-Arevalo, J.M., Garcia-Mayordomo, J., 2007. Tectonic and climatic control on the dissolution of limestone profiles in the Sierra Morena (Southern Iberia). *Geodinamica Acta* 20, 1–12.
- Herrero, M.J., Insua-Arevalo, J.M., Garcia-Mayordomo, J., 2006. Tectonic and climatic control on the dissolution of limestone profiles in the Sierra Morena (Southern Iberia). *Geodinamica Acta* 19, 1–12.
- Herrero, M.J., Insua-Arevalo, J.M., Garcia-Mayordomo, J., 2005. Tectonic and climatic control on the dissolution of limestone profiles in the Sierra Morena (Southern Iberia). *Geodinamica Acta* 18, 1–12.
- Herrero, M.J., Insua-Arevalo, J.M., Garcia-Mayordomo, J., 2004. Tectonic and climatic control on the dissolution of limestone profiles in the Sierra Morena (Southern Iberia). *Geodinamica Acta* 17, 1–12.
- Herrero, M.J., Insua-Arevalo, J.M., Garcia-Mayordomo, J., 2003. Tectonic and climatic control on the dissolution of limestone profiles in the Sierra Morena (Southern Iberia). *Geodinamica Acta* 16, 1–12.
- Herrero, M.J., Insua-Arevalo, J.M., Garcia-Mayordomo, J., 2002. Tectonic and climatic control on the dissolution of limestone profiles in the Sierra Morena (Southern Iberia). *Geodinamica Acta* 15, 1–12.
- Herrero, M.J., Insua-Arevalo, J.M., Garcia-Mayordomo, J., 2001. Tectonic and climatic control on the dissolution of limestone profiles in the Sierra Morena (Southern Iberia). *Geodinamica Acta* 14, 1–12.
- Herrero, M.J., Insua-Arevalo, J.M., Garcia-Mayordomo, J., 2000. Tectonic and climatic control on the dissolution of limestone profiles in the Sierra Morena (Southern Iberia). *Geodinamica Acta* 13, 1–12.
- Herrero, M.J., Insua-Arevalo, J.M., Garcia-Mayordomo, J., 1999. Tectonic and climatic control on the dissolution of limestone profiles in the Sierra Morena (Southern Iberia). *Geodinamica Acta* 12, 1–12.
- Herrero, M.J., Insua-Arevalo, J.M., Garcia-Mayordomo, J., 1998. Tectonic and climatic control on the dissolution of limestone profiles in the Sierra Morena (Southern Iberia). *Geodinamica Acta* 11, 1–12.
- Herrero, M.J., Insua-Arevalo, J.M., Garcia-Mayordomo, J., 1997. Tectonic and climatic control on the dissolution of limestone profiles in the Sierra Morena (Southern Iberia). *Geodinamica Acta* 10, 1–12.
- Herrero, M.J., Insua-Arevalo, J.M., Garcia-Mayordomo, J., 1996. Tectonic and climatic control on the dissolution of limestone profiles in the Sierra Morena (Southern Iberia). *Geodinamica Acta* 9, 1–12.
- Herrero, M.J., Insua-Arevalo, J.M., Garcia-Mayordomo, J., 1995. Tectonic and climatic control on the dissolution of limestone profiles in the Sierra Morena (Southern Iberia). *Geodinamica Acta* 8, 1–12.
- Herrero, M.J., Insua-Arevalo, J.M., Garcia-Mayordomo, J., 1994. Tectonic and climatic control on the dissolution of limestone profiles in the Sierra Morena (Southern Iberia). *Geodinamica Acta* 7, 1–12.
- Herrero, M.J., Insua-Arevalo, J.M., Garcia-Mayordomo, J., 1993. Tectonic and climatic control on the dissolution of limestone profiles in the Sierra Morena (Southern Iberia). *Geodinamica Acta* 6, 1–12.
- Herrero, M.J., Insua-Arevalo, J.M., Garcia-Mayordomo, J., 1992. Tectonic and climatic control on the dissolution of limestone profiles in the Sierra Morena (Southern Iberia). *Geodinamica Acta* 5, 1–12.
- Herrero, M.J., Insua-Arevalo, J.M., Garcia-Mayordomo, J., 1991. Tectonic and climatic control on the dissolution of limestone profiles in the Sierra Morena (Southern Iberia). *Geodinamica Acta* 4, 1–12.
- Herrero, M.J., Insua-Arevalo, J.M., Garcia-Mayordomo, J., 1990. Tectonic and climatic control on the dissolution of limestone profiles in the Sierra Morena (Southern Iberia). *Geodinamica Acta* 3, 1–12.
- Herrero, M.J., Insua-Arevalo, J.M., Garcia-Mayordomo, J., 1989. Tectonic and climatic control on the dissolution of limestone profiles in the Sierra Morena (Southern Iberia). *Geodinamica Acta* 2, 1–12.
- Herrero, M.J., Insua-Arevalo, J.M., Garcia-Mayordomo, J., 1988. Tectonic and climatic control on the dissolution of limestone profiles in the Sierra Morena (Southern Iberia). *Geodinamica Acta* 1, 1–12.

http://www.ub.edu/~jmherrero/Calcareous_Fault.html

jmherrero@ub.edu

http://www.ub.edu/~jmherrero/Calcareous_Fault.html

jmherrero@ub.edu





Tectonics

RESEARCH ARTICLE

10.1002/2015TC003997

Key Points:

- Paleoseismicity in the Eastern Betic Shear Zone (Carrascoy Fault SW segment)
- Migration of active faulting away from the main range (foreberg)
- Nine to 11 M_w ~6.7 events in the last 30.2 kyr and a slip rate of 0.37 m/kyr

Supporting Information:

- Tables S1–S5 captions
- Table S1
- Table S2
- Table S3
- Table S4
- Table S5

Correspondence to:

R. Martín-Banda,
raquem@ucm.es

Citation:

Martín-Banda, R., J. García-Mayordomo, J. M. Insua-Arévalo, A. E. Salazar, E. Rodríguez-Escudero, J. A. Álvarez-Gómez, A. Mediadea, and M. J. Herrero (2016), New insights on the seismogenic potential of the Eastern Betic Shear Zone (SE Iberia): Quaternary activity and paleoseismicity of the SW segment of the Carrascoy Fault Zone, *Tectonics*, 35, 55–75, doi:10.1002/2015TC003997.

Received 10 AUG 2015

Accepted 24 NOV 2015

Accepted article online 26 NOV 2015

Published online 6 JAN 2016

New insights on the seismogenic potential of the Eastern Betic Shear Zone (SE Iberia): Quaternary activity and paleoseismicity of the SW segment of the Carrascoy Fault Zone

Raquel Martín-Banda¹, Julián García-Mayordomo², Juan M. Insua-Arévalo¹, Ángel E. Salazar², Emilio Rodríguez-Escudero³, Jose A. Álvarez-Gómez¹, Alicia Mediadea⁴, and María J. Herrero⁵

¹Department of Geodynamics, Complutense University of Madrid, Madrid, Spain, ²Geological and Mining Institute of Spain, Madrid, Spain, ³Department of Geology and Geochemistry, Autónoma University of Madrid, Madrid, Spain, ⁴Nordic Laboratory for Luminescence Dating, Department of Geoscience, Aarhus University, Aarhus, Denmark, ⁵Department of Petrology and Geochemistry, Complutense University of Madrid, Madrid, Spain

Abstract The Carrascoy Fault (CAF) is one of the main active faults that form part of the Eastern Betic Shear Zone, a 450 km fault system that accommodates most of the convergence between the Eurasian (Iberia) and Nubian plates in the Betic Cordillera, south Spain. Although the CAF represents a major earthquake threat to the nearby City of Murcia, studies on its Quaternary tectonics and seismogenic potential are scarce to date. We present evidence that supports the division of the CAF into two overlapping segments with contrasting tectonic structure, Quaternary activity, and landform control: a SW segment, characterized by a broad fold-and-thrust zone similar to the forebergs defined in the Gobi-Altai region, and a NE segment, characterized by a sharp mountain front controlled by strike-slip tectonics. We attribute the differentiation into these two segments to the stresses associated with topography, which in turn is a consequence of the shortening component, at the middle Pleistocene, after circa 217.4 ka. For the SW segment we infer the occurrence of 9 to 11, M_w ~6.7 paleoearthquakes in the last 30.2 kyr, and a slip rate of 0.37 ± 0.08 m/kyr. We date the occurrence of the last surface rupture event after 2750 B.P., and we estimate an average recurrence period of major events of 3.3 ± 0.7 kyr.

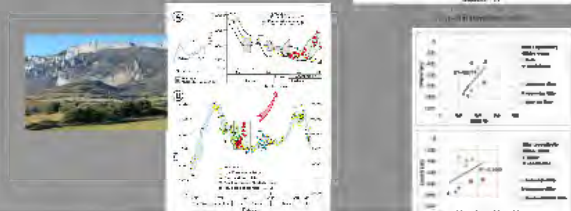
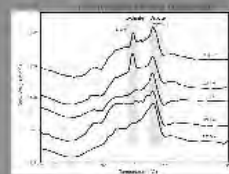
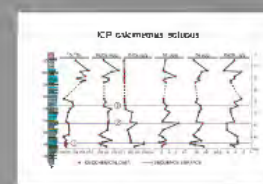
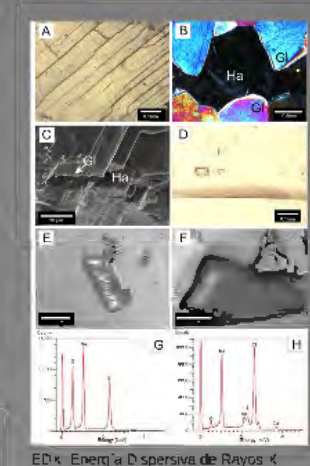
1. Introduction

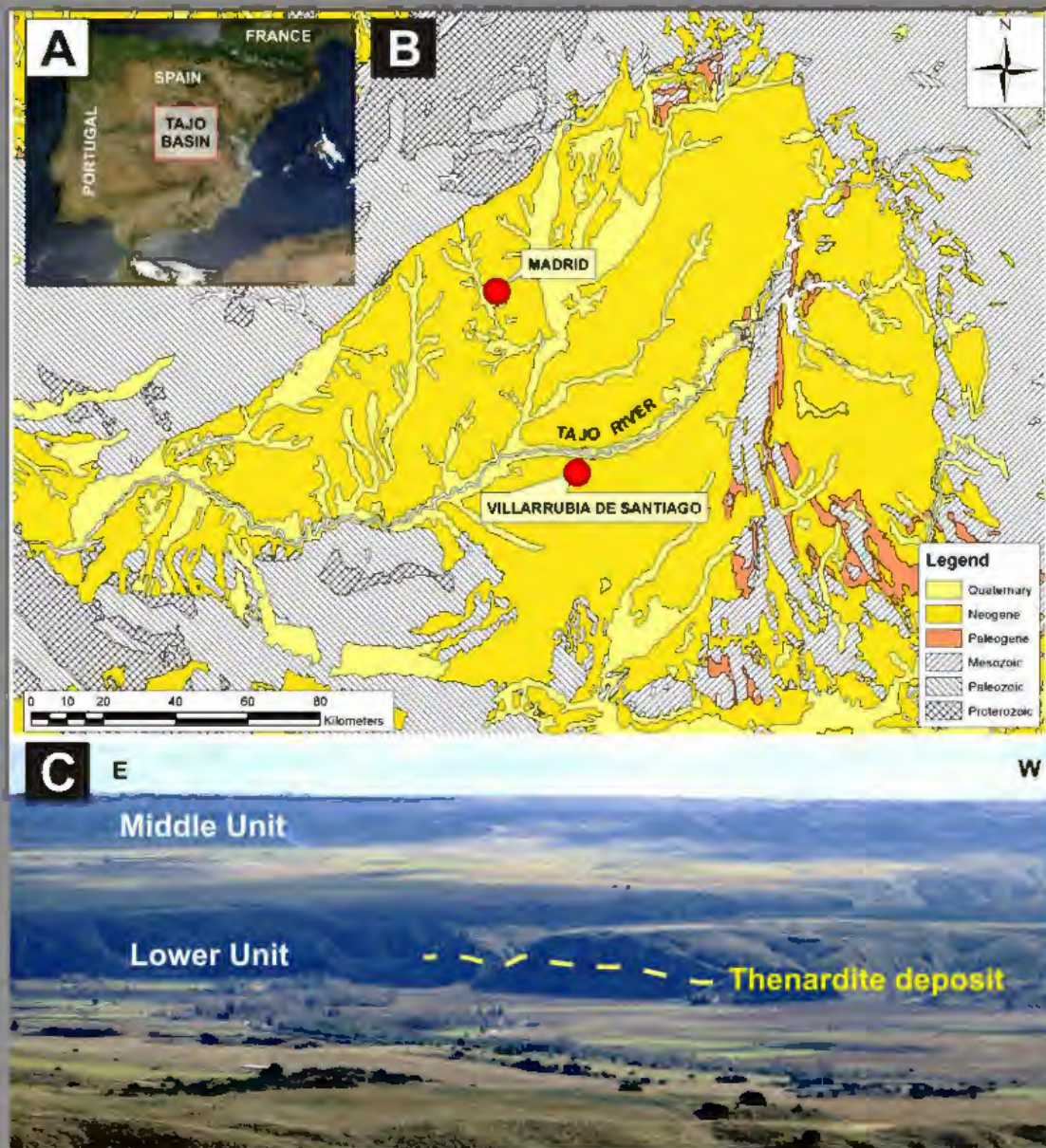
The Eastern Betic Shear Zone (EBSZ) is the main fault system accommodating the convergence between the Eurasian and Nubian plates in Iberia since late Neogene [Bousquet, 1979; De Larouzière *et al.*, 1988; Sanz de Galdeano, 1990; Silva *et al.*, 1993]. It shows a characteristic sigmoidal shape extending for more than 450 km from offshore Alboran Sea to NE of Murcia (Figure 1). Along the EBSZ many destructive earthquakes have taken place since historical times proving the seismogenic behavior of the faults that form the shear zone. From southwest to northeast, the EBSZ is formed by the following main faults: Carboneras, Palomares, Alhama de Murcia, Carrascoy, and Bajo Segura [Instituto Geológico y Minero de España (IGME), 2012].

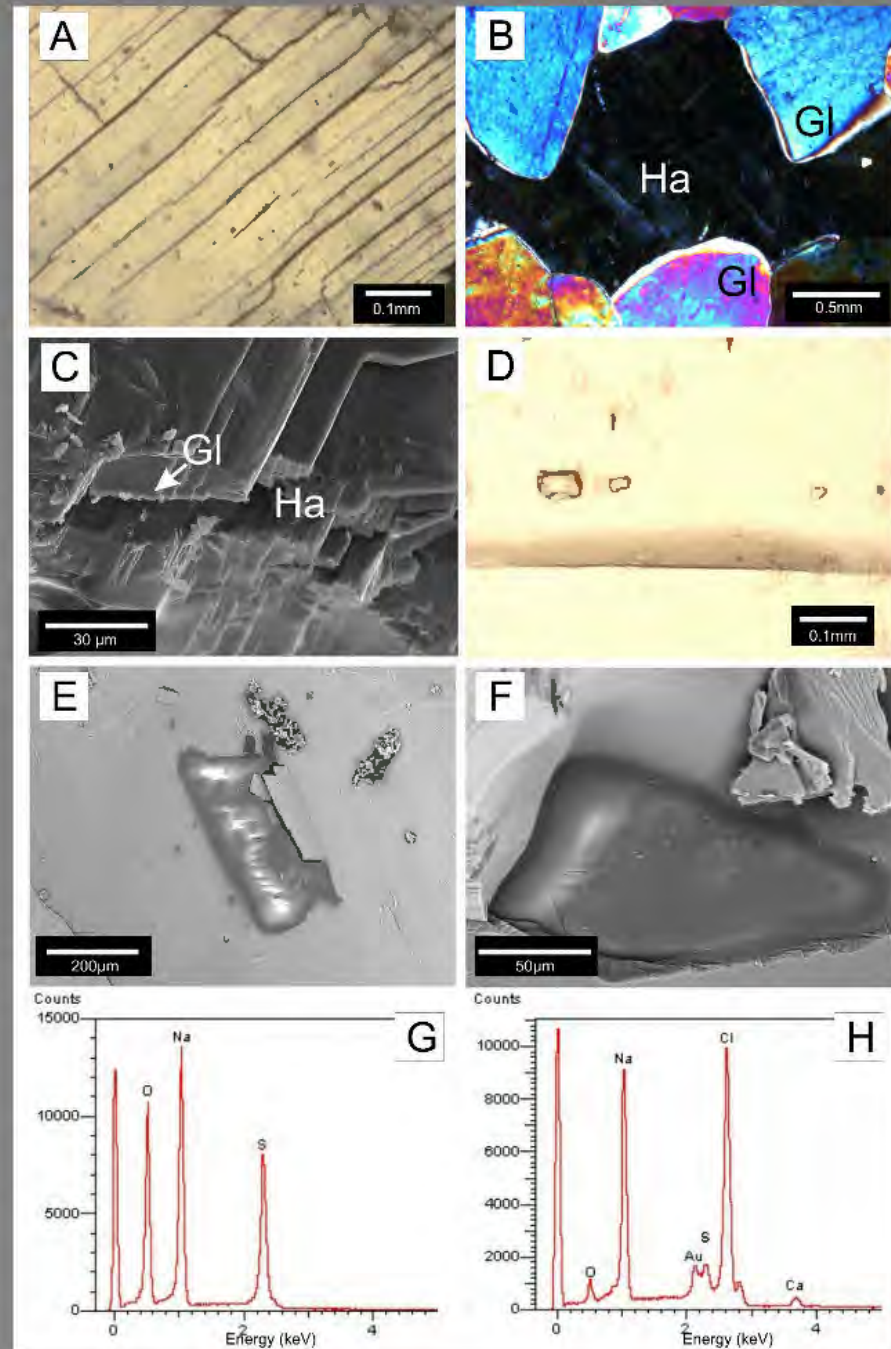
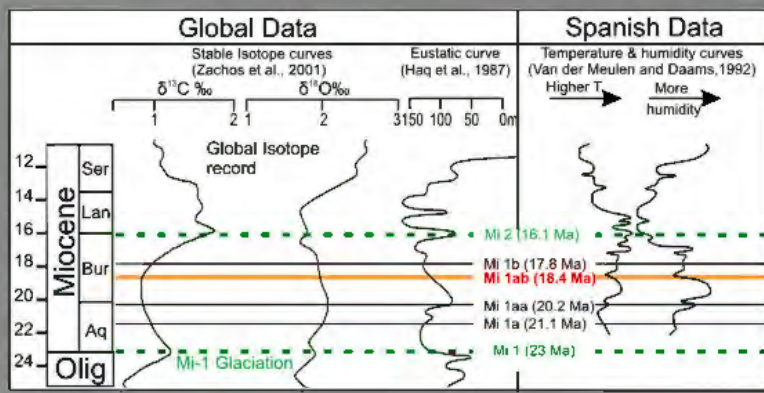
The Quaternary activity of the faults that form the EBSZ has been noticed and studied since the end of the 1970s decade [e.g., Bousquet, 1979; Sanz de Galdeano, 1983; Boccaletti *et al.*, 1987; Montenat *et al.*, 1987; Vegas *et al.*, 1987; Masana *et al.*, 2010; Buontempo and Wuestefeld, 2013]. Furthermore, most of these faults have been also studied from a paleoseismological point of view: Carboneras [e.g., Bell *et al.*, 1997; Moreno *et al.*, 2008; Moreno, 2010], Alhama de Murcia [e.g., Hernández-Enrile and Martínez-Díaz, 2001; Ortúñoz *et al.*,



Del Clima del Pasado al Clima del Futuro

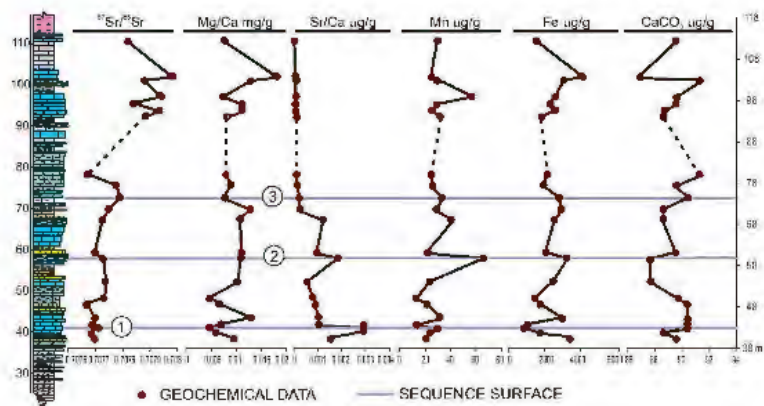




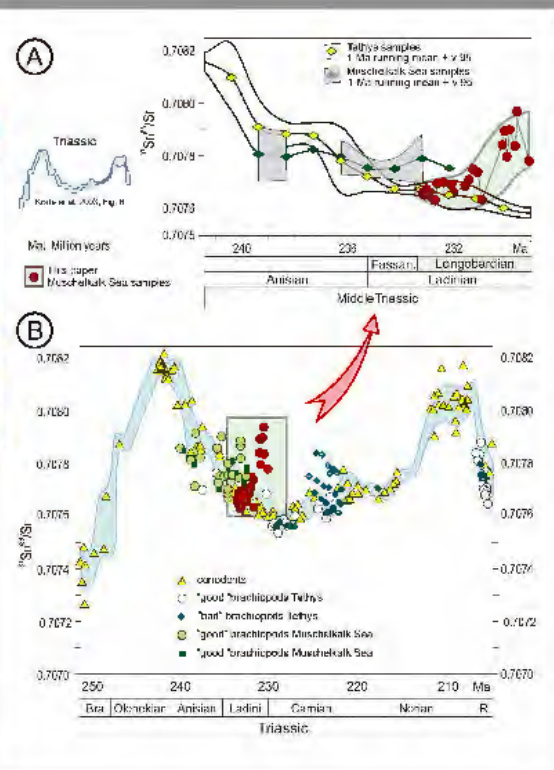
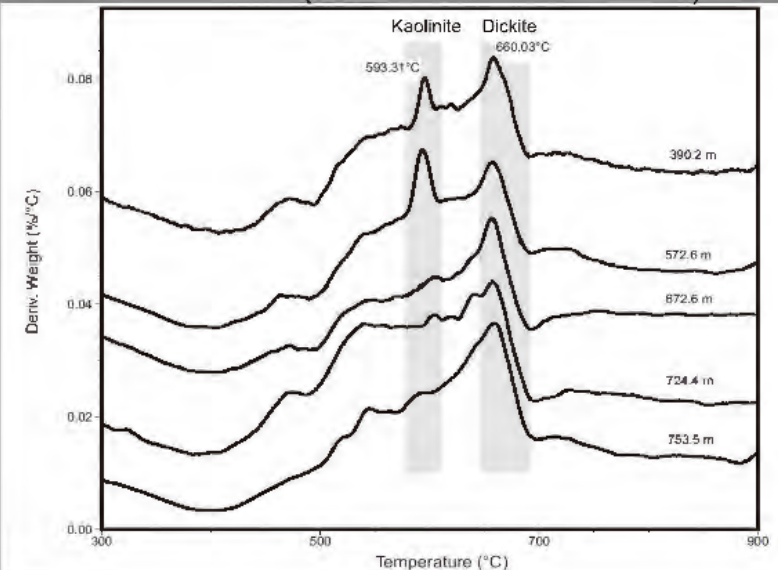


EDX: Energía Dispersiva de Rayos X

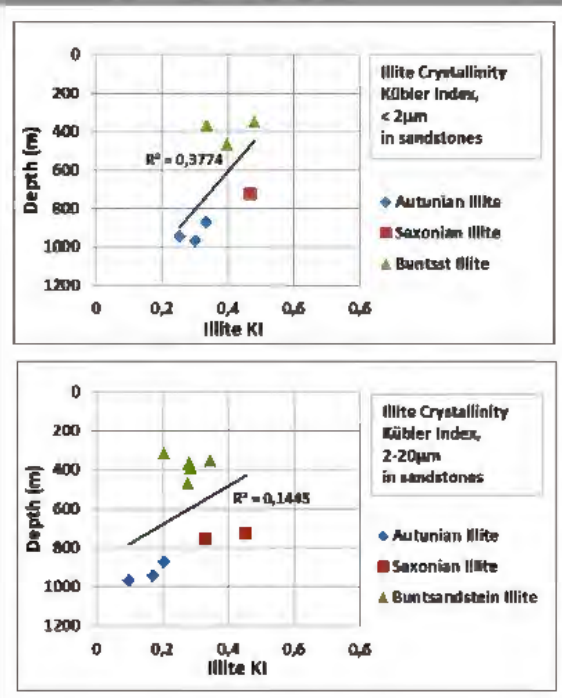
ICP, calcimetrias isótopos

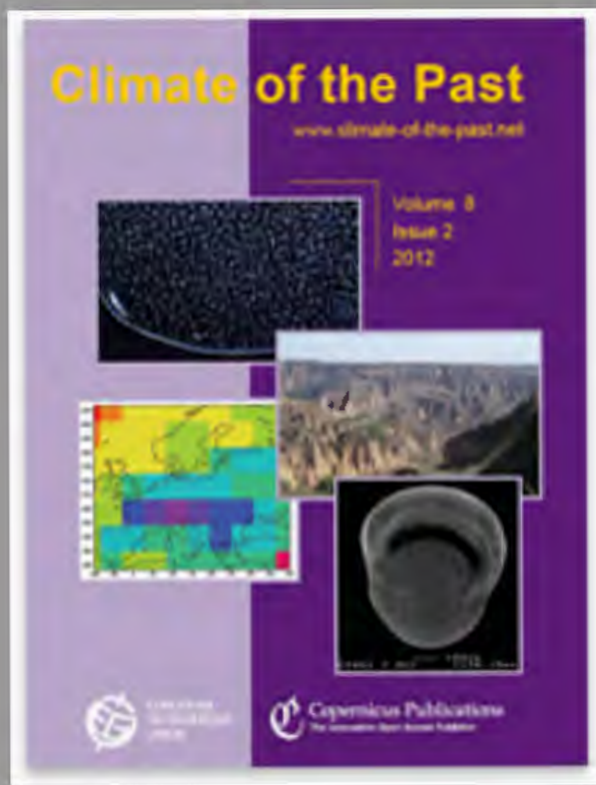


ATD (Análisis Térmico Diferencial)



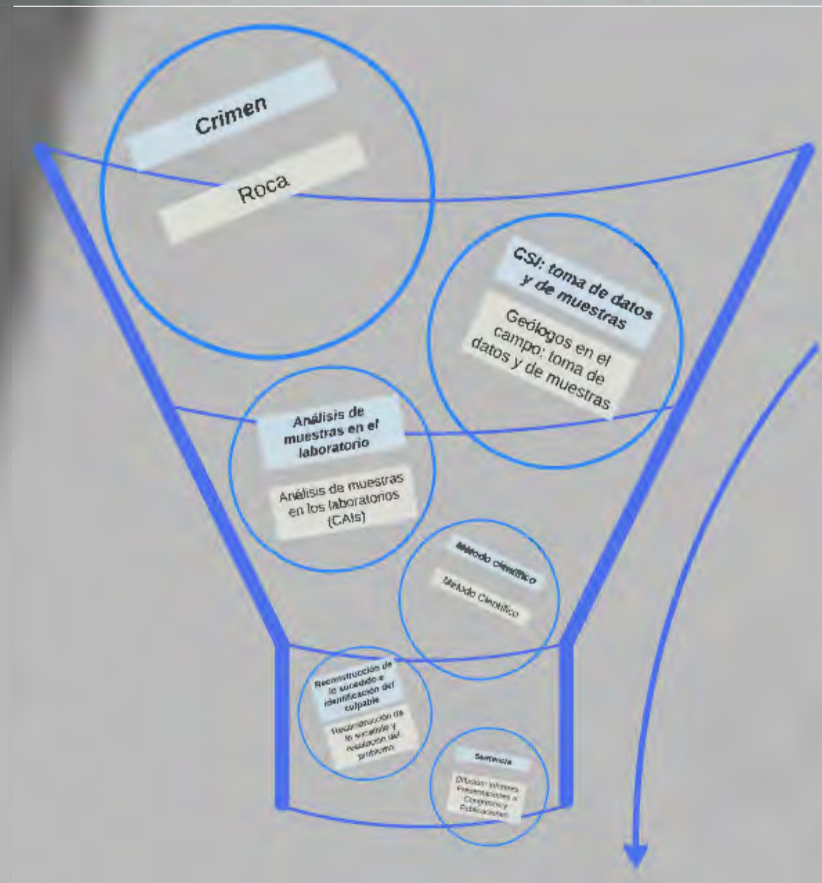
Cristalinidad de la Illita



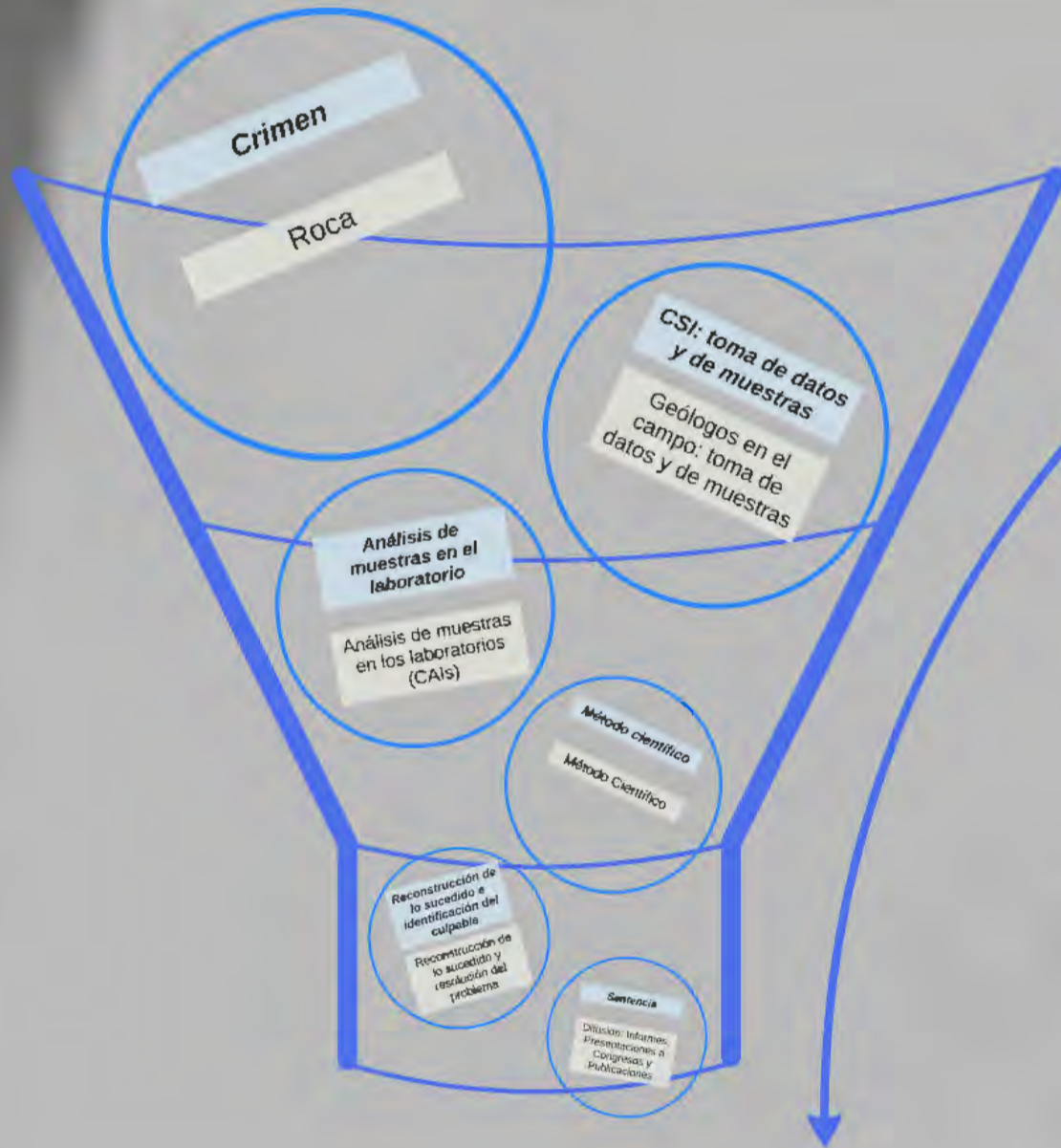


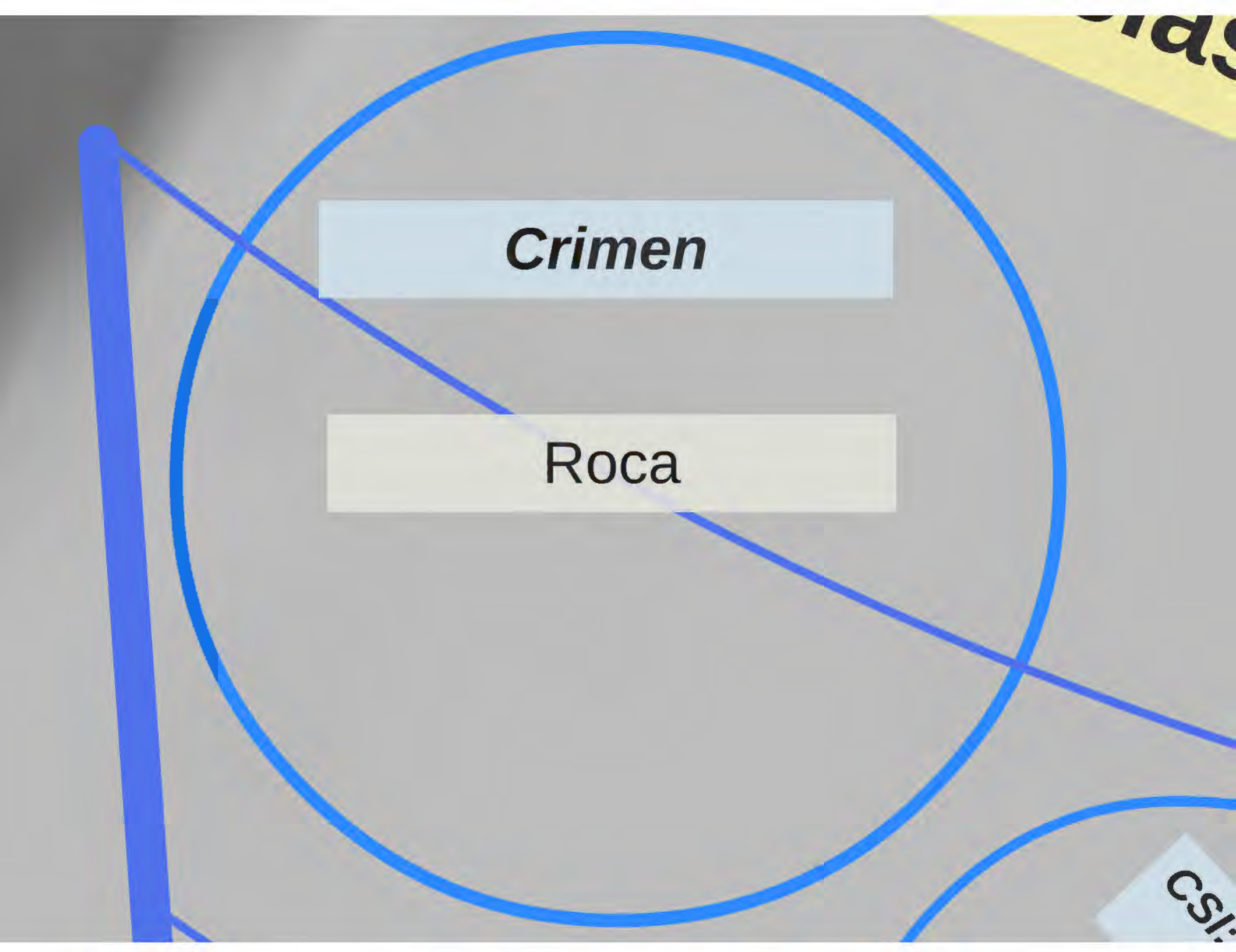


Investigación Aplicada en Ciencias de la Tierra



Investigación Aplicada en Ciencias de la Tierra





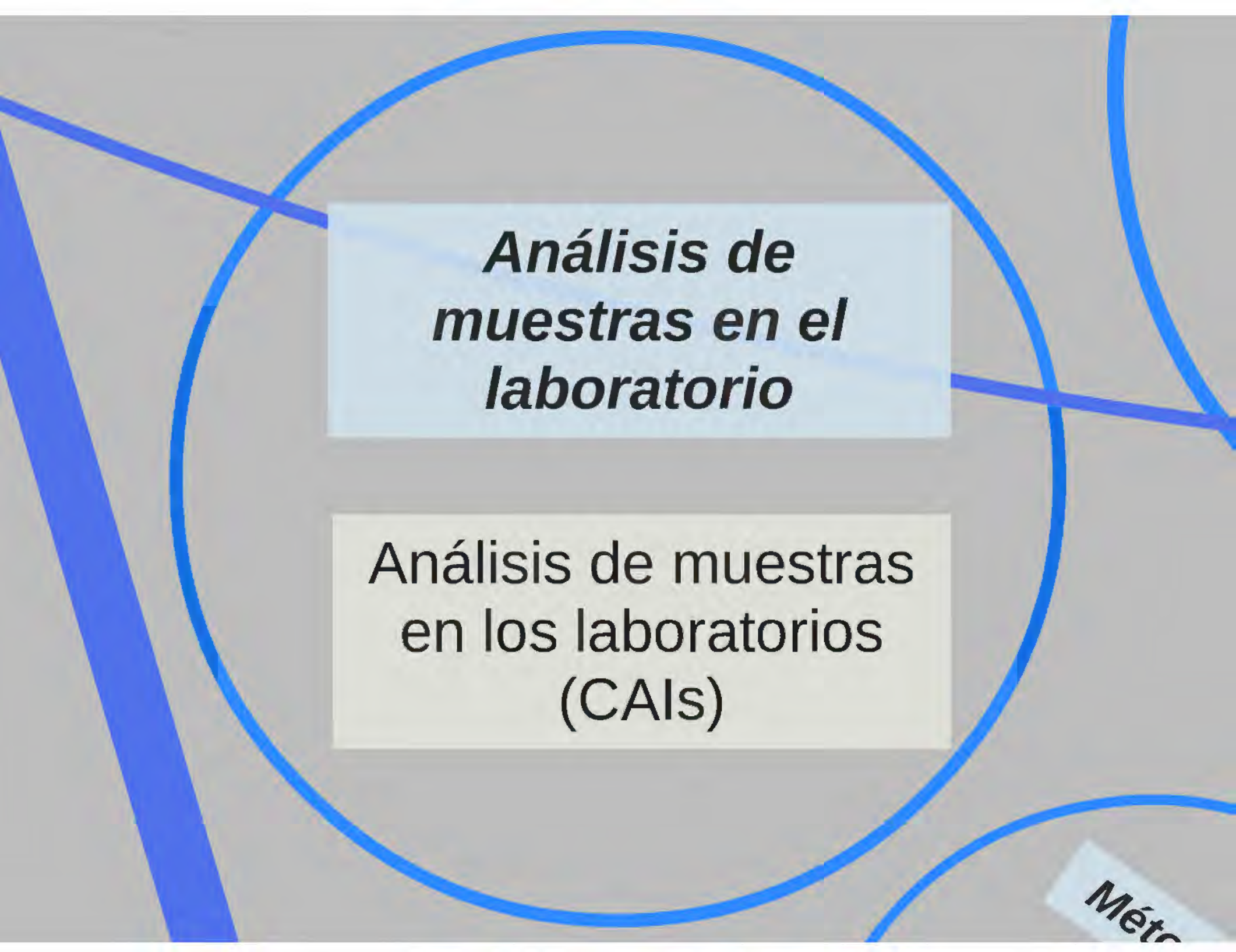
Crimen

Roca

CSL

CSI: toma de datos y de muestras

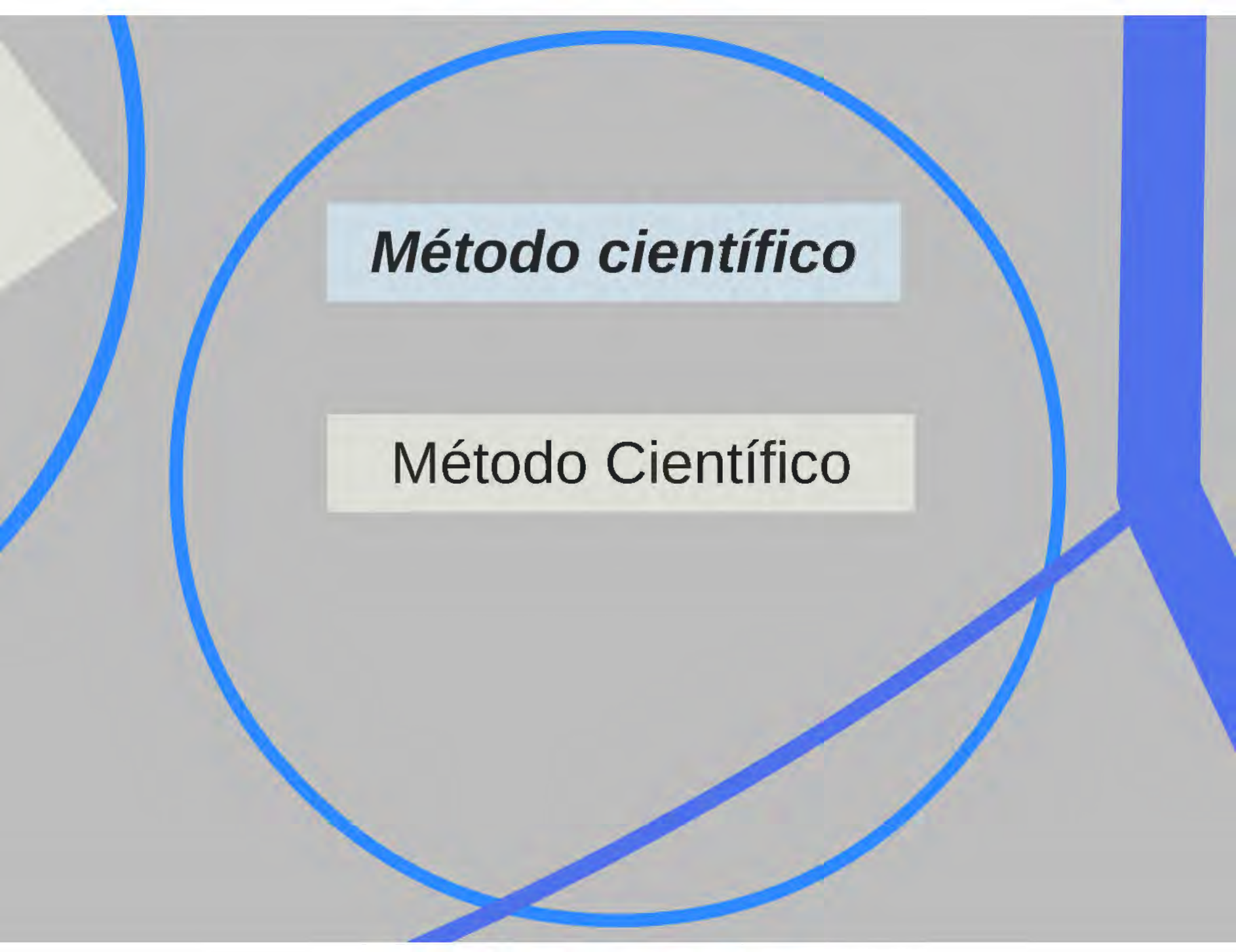
Geólogos en el
campo: toma de
datos y de muestras



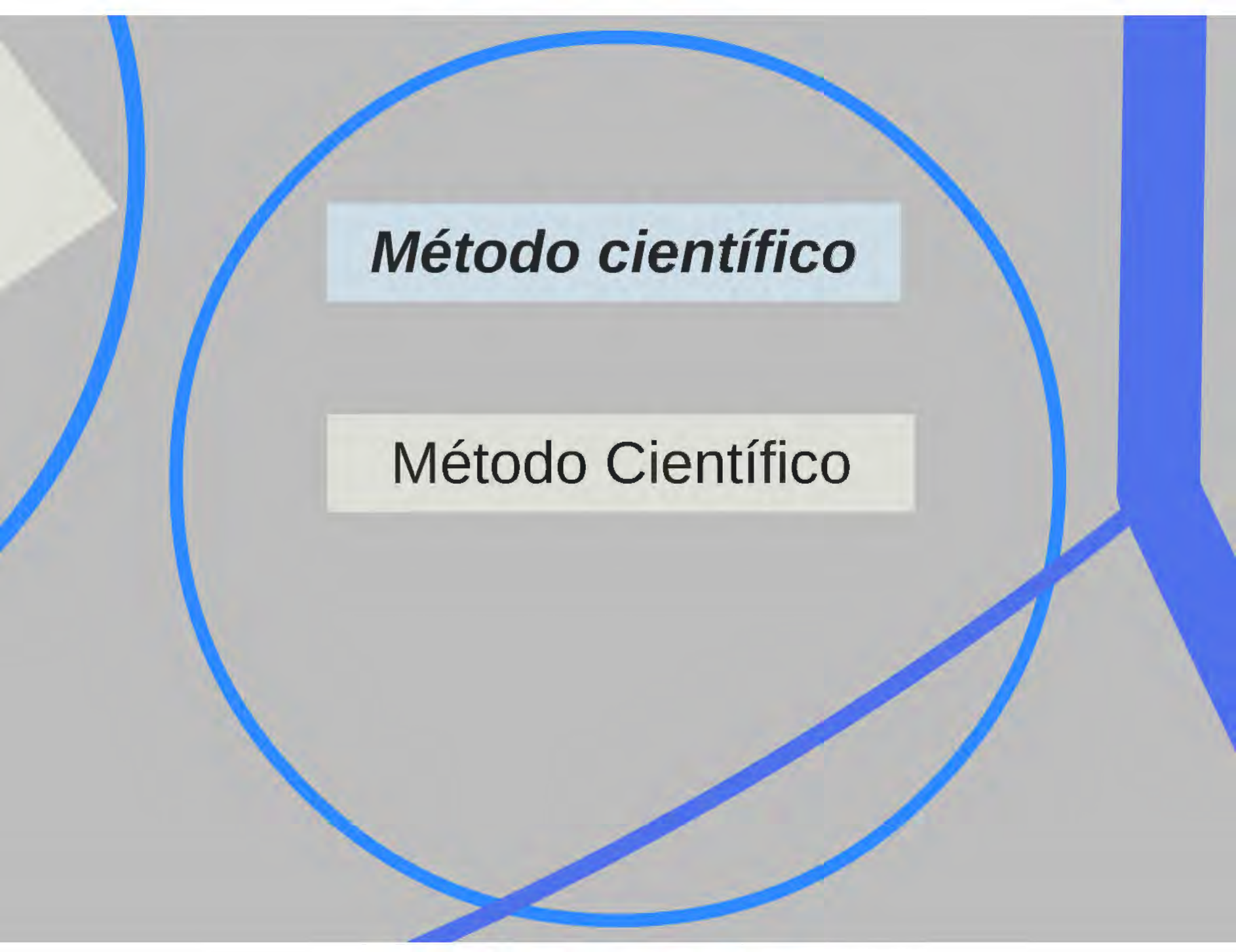
Análisis de muestras en el laboratorio

Análisis de muestras
en los laboratorios
(CAIs)

Méto



Método científico



Método Científico

***Reconstrucción de
lo sucedido e
identificación del
culpable***

Reconstrucción de
lo sucedido y
resolución del
problema

Sentencia

Difusión: Informes,
Presentaciones a
Congresos y
Publicaciones

GRACIAS